


Cell culture models of oral mucosal barriers: A review with a focus on applications, culture conditions and barrier properties

Lisa Bierbaumer^{a*}, Uwe Yacine Schwarze ^{b,c}, Reinhard Gruber ^{b,c,d}, and Winfried Neuhaus ^a

^aCompetence Unit Molecular Diagnostics, Center Health and Bioresources, Austrian Institute of Technology (AIT) GmbH, Vienna, Austria; ^bDepartment of Oral Biology, School of Dentistry, Medical University of Vienna, Vienna, Austria; ^cAustrian Cluster for Tissue Regeneration, Vienna, Austria; ^dDepartment of Periodontology, School of Dental Medicine, University of Bern, Bern, Switzerland

ABSTRACT

Understanding the function of oral mucosal epithelial barriers is essential for a plethora of research fields such as tumor biology, inflammation and infection diseases, microbiomics, pharmacology, drug delivery, dental and biomarker research. The barrier properties are comprised by a physical, a transport and a metabolic barrier, and all these barrier components play pivotal roles in the communication between saliva and blood. The sum of all epithelia of the oral cavity and salivary glands is defined as the blood-saliva barrier. The functionality of the barrier is regulated by its microenvironment and often altered during diseases. A huge array of cell culture models have been developed to mimic specific parts of the blood-saliva barrier, but no ultimate standard *in vitro* models have been established. This review provides a comprehensive overview about developed *in vitro* models of oral mucosal barriers, their applications, various cultivation protocols and corresponding barrier properties.

ARTICLE HISTORY

Received 15 May 2018
Accepted 17 May 2018

KEYWORDS

saliva; tight junctions; desmosomes; ABC-transporters; SLC-transporter; craniomaxillofacial surgery; salivary gland; tongue; gingivitis; periodontitis

Introduction

Ever since evolution allowed for cell type specialization and compartmentalization, the formation of biological barriers gained specific importance. The major interfaces between an organism and the external environment or between different compartments are made up of organized and continuous epithelial cell sheets. Important barrier-forming epithelia are building up the epidermis, the surfaces of the eyes, the surfaces of the digestive, respiratory, reproductive and urinary tracts and the ducts and secretory cells of different glands.¹ Depending on their location, epithelia accomplish several critical functions. Concretely, they play a major role in maintaining homeostasis and act as selective filters that regulate the trans-cellular movement of solutes between different compartments.² At the same time, they can act as barriers to protect underlying tissue from physical and chemical damage, bacterial infection, dehydration or heat loss.³ The physical barrier aspect of epithelia is defined by the cell membrane and cell junctions that tightly connect neighbor cells to

each other and thereby regulate the movement of substances via the paracellular way. In addition, epithelial cell layers represent a transport barrier using influx as well as efflux proteins (transporter proteins or receptors) for small molecules as well as proteins and a metabolic barrier applying enzymes for the modification or conversion of molecules.

Studies on barrier functionality of several epithelial subtypes have shown that cellular barriers are no static constructs, but that they can be altered by several conditions. As an example, it is well known that inflammation and the release of proinflammatory cytokines such as interferon- γ (INF γ) and tumor necrosis factor- α (TNF α) lead to compromised permeability in *in vitro* models, e.g. for intestinal mucosa⁴⁻⁶ or salivary glands.⁷⁻⁹

Next to epithelial cell sheets, another example of an extensively studied biological barrier is the blood-brain barrier (BBB), which main component are brain capillary endothelial cells. In cooperation with other cell types such as astrocytes, pericytes or neurons, the BBB acts as a bidirectional filter controlling the exchange of substances at the

CONTACT Winfried Neuhaus  winfried.neuhaus@ait.ac.at

*Current affiliation: Children's Cancer Research Institute (CCRI), Molecular Biology of Solid Tumors, Zimmermannplatz 10, 1090 Vienna, Austria.

© 2018 The Author(s). Published with license by Taylor & Francis. This is an Open Access article distributed under the terms of the Creative Commons Attribution-NonCommercial-NoDerivatives License (<http://creativecommons.org/licenses/by-nc-nd/4.0/>), which permits non-commercial re-use, distribution, and reproduction in any medium, provided the original work is properly cited, and is not altered, transformed, or built upon in any way.

interface of the blood and the fluids of the central nervous system (CNS).¹⁰

In contrast to other well characterized biological barriers such as the BBB, the gastrointestinal tract or pulmonary epithelia, less research has been done on cellular barriers which separate blood compartments from saliva. This blood-saliva barrier (BSB) is mainly defined by epithelia of the oral cavity and salivary glands. In addition to epithelial cells, these cell layers are infiltrated by other cell types such as Langerhans cells, melanocytes, Merkel cells or endothelial cells forming blood vessels that might contribute to barrier functionality.

Modelling epithelia of the oral and salivary glands *in vitro* by cell monolayers and complex tissue engineering approaches has been a major goal of recent studies. A plethora of *in vitro* models of the BSB has been developed, but no ultimate, standardized models are established neither for models of the oral cavity nor for salivary gland epithelia. Moreover, the epithelia of different regions in the oral cavity (tongue, gingiva, buccal) exhibit significant different barrier properties.¹¹ This is also valid for epithelia from salivary glands (acini, ductal cells). In addition, differences between the three major salivary glands (*glandula submandibularis*, *parotis* and *sublingualis*) as well as the hundreds of minor salivary glands are probable. A minority of the studies using *in vitro* BSB models are dealing with transport processes of molecules across the BSB. A prerequisite to interpret these reports properly is to understand the barrier properties of these models, which are also understudied. Moreover, cell culture conditions (growth medium, supplements, cell seeding density; submerged *versus* air-lift set-up, cell type and origin, mono – or multicultures, 2D or 3D) distinctly influence the resulting barrier properties of the used *in vitro* models. Therefore, there was an essential need for a comprehensive summary considering all the different parameters for *in vitro* models of the BSB, on the one hand to provide a general overview for readers who are interested in the topic, but also for researchers who apply and would like to compare or improve their *in vitro* models. The first chapter deals generally with transport routes across epithelial cell layers in relation to the BSB with some examples, the second

chapter describes how the barrier functionality is assessed in *in vitro* models. These two chapters provide the fundamentals in order to understand and classify the data presented in chapters three and four about barrier studies with *in vitro* models of the epithelia of the oral cavity and the salivary glands. Each of these two chapters begins with a short anatomical overview and general considerations, before the detailed data about the *in vitro* models are presented and discussed.

Transport Routes across Epithelial Cell Layers

In general, permeation across epithelial barriers is largely achieved by simple passive diffusion (mostly paracellular), carrier-mediated diffusion, active transport or endocytosis.¹² The transport route is mainly determined by lipophilicity, charge and overall molecular geometry of the permeant.¹² For buccal mucosa, it is thought that the majority of tracers and peptide drugs is transported through the paracellular route by passive diffusion.^{13,14}

Transporter proteins

Active transport of xenobiotics via membrane transporters is an important aspect for the development of alternative drug delivery routes such as transbuccal drug transport, as they can determine pharmacokinetic, safety and efficacy profiles of drugs.¹⁵ During recent years, two major superfamilies of membrane transporters have been extensively studied, namely ATP-binding cassette (ABC) and solute carrier (SLC) transporters. They are key regulators that manage the movement of endogenous metabolites maintaining physiological homeostasis as well as xenobiotics such as drugs and toxins.¹⁶ To date, more than 400 ABC and SLC members have been identified in the human genome with expression patterns throughout the whole body.^{15,17} Most notably, expression of both transporter families has been detected in barrier-forming epithelia of major organs such as kidney, liver, intestine, placenta and eye, as well as other body fluid-separating compartments such as the BBB.^{18–23} On the mechanistic level, both transporter families act differently. ABC members represent ATP-dependent efflux transporters in all living organisms,

whereas the ABC importer function seems to be restricted to prokaryotes.²⁴ In contrast, SLC members are mainly uptake transporters that do not rely on ATP hydrolysis.¹⁷ SLC and ABC transporters have been described to be polyspecific, i.e. to transport several substrates with different affinities and regulations in distinct tissues. Furthermore, membrane transporters show overlapping substrate specificities among the ABC and SLC superfamilies.²¹ Many ABC and SLC members have been described to be clinically relevant with several gene polymorphism linked to diseases (for reviews see e.g.,^{17,21,25,26,27}). However, the study of SLC transporters can be hindered using *in vitro* models, as many cell lines at higher passages lose transporter expression and activity.¹⁷

Considering BSB compartments, current data suggest that active transport across buccal mucosa seems to be rare.²⁸ In this context, active transport processes have not been extensively studied across the BSBs and therefore the endogenous function of these transporters are not well understood. Therefore, comprehensive investigations of active transport mechanisms across the BSB are still missing and their results might change the current view about their relevance for BSB functionality.

Cell junctions

The paracellular barrier functionality of polarized epithelia is strongly determined by tight junctions (TJs), adherens junctions (AJs) and desmosomes, which are the main constituents of a multiprotein complex referred to as apical junctional complex (AJC) located at the most apical end of the lateral plasma membrane.²⁹ Primarily, TJs act as paracellular gates that restrict diffusion of ions and solutes based on their molecular size and charge.³⁰ In epithelial cell layers, TJs consist of a narrow belt-like structure in the apical region of the lateral plasma membrane. TJs are found in tissues that are involved in polarized secretions, absorption functions, and maintaining barriers between blood and interstitial fluids. The proteins sealing the paracellular gaps belong to the claudin family. Currently, over 20 members of the human claudin family have been identified.³¹ Claudins can bind to other claudins of the neighbor cell either in a homo- or a heteromeric manner. Other proteins

important for the structure of the TJs are occludin or tricellulin as well as the group of the junctional adhesion molecules (JAMs). Importantly, the extracellular parts of the TJs are linked via tight-junction associated proteins such as zonula occludens (ZO) 1 to 3 to the cytoskeleton enabling a direct signaling from outside the cells into the cytosol.³² The expression of TJ proteins is mostly investigated either by PCR or Western blot analysis at the mRNA or protein level. In order to understand changes on the functional level, permeability studies with paracellular marker molecules are accomplished and supported by imaging analysis to visualize the localization of TJ proteins. Many authors use TEM for ultrastructural analysis to ensure the distribution of TJ within the cell layers.^{33,34} In the case of BSB models, some approaches have been made, but still no comprehensive studies were accomplished to understand the complex tight junction network of BSB models investigating it at the expression, at the localization and the functional level. The stratum corneum is the topmost additional and specialized layer which contributes to the paracellular barrier of the stratified parts of the oral mucosa. Lamellar bodies or so-called membrane coating granules are formed and released by keratinizing epithelial cells during the differentiation processes. These granules contain lipids (e.g. glucosylceramides), hydrolytic enzymes and proteins (e.g. corneodesmosin), which are released after the secretion of the granules and spread over the cell surfaces to support the formation of a thick cell envelope resistant against keratinolytic agents.^{35,36} This cell envelope is water-impermeable and a very strong shield preventing paracellular permeability in keratinized stratified squamous epithelia of the oral mucosa. On the contrary, in non-stratified epithelial layers tight junctions might form the major paracellular barrier.

Endocytosis

In order to internalize molecules from the extracellular space, cells also use endocytic processes, where cargo material is engulfed by an invagination of the plasma membrane. In general, two main types of endocytosis are classified depending on the size of ingested material and in the following of formed endocytic vesicles.

The ingestion of larger particles such as microorganisms is accomplished by phagocytosis, which is most efficiently performed by specialized phagocytic cells. In contrast, pinocytosis allows for the uptake of fluids and small solutes.³⁷ Endocytosis could be mediated via receptors or adsorption (onto the cellular surface due to electrostatic interactions). For example, multiple mechanisms for the internalization of *Candida albicans* or HIV in oral epithelial cells were shown. Fungal invasins derived from *Candida albicans* stimulated epidermal growth factor receptor which caused rearrangement of the epithelial microfilaments and the formation of pseudopods taking up the fungus into the epithelial cells. In case of HIV, several pathways such as clathrin-, caveolin/lipid raft-associated endocytosis and micropinocytosis were involved in the epithelial uptake of the virus^{38,39,40} The transferrin receptor (TfR) is another receptor relevant for endocytosis at the oral epithelium. TfR was used as a marker for oral epithelial cells and was reported to mediate the uptake of *Porphyromonas gingivalis*, a well-known periodontal pathogen. Some drug delivery strategies tried to exploit receptor-mediated endocytosis. For example, nanoparticles decorated with transferrin aimed at binding to the transferrin receptor and to increase the uptake of these nanoparticles via TfR-mediated endocytosis into epithelial cells.^{41,42,43} In this context, endocytic transport processes have not been extensively studied across the BSBs and comprehensive investigations of endocytosis at the BSB are still missing.

In terms of barrier functionality, endocytic processes have been described to be involved in TJ regulation by AJC internalization, which results in the reversible opening of epithelial barriers or alteration of cell-cell adhesion properties.⁴⁴ Several pathogenic stimuli such as cytokines, growth factors, oxidative stress and bacterial or viral toxins have been shown to be strong inducers of cytosolic translocation of AJ as well as TJ proteins.⁴⁴ For example, proinflammatory IFN- γ was described to increase paracellular permeability in the T84 intestinal epithelial cell model by inducing endocytosis of the TJ proteins occludin, JAM-A and claudin-1, concretely via myosin II-dependent vacuolarization of the apical plasma membrane.⁴⁵ Studies performed by Harhaj *et al.* showed that PDGF altered permeability and TJ distribution in MDCK cells, most likely including

the endosomal pathway.⁴⁶ Another example for endocytosis-inducing effects is *Escherichia coli*'s toxin cytotoxic necrotizing factor-1 (CNF-1) that enhanced paracellular permeability across intestinal epithelial monolayers and arranged TJ protein redistribution essential for epithelial barrier functionality.⁴⁷ However, redistribution of several cadherins through distinct endocytic pathways not only leads to pathological processes, but also is a key mechanism during development and tissue patterning.⁴⁸

Mucus as an additional barrier

It is generally recognized that also extracellular components contribute to the barrier function of many epithelia. As an example, the lipid matrix composition plays an important role in the paracellular diffusion pathway, especially when the compounds such as peptides are hydrophilic or have high molecular weights. In addition, all mucosal surfaces throughout the body are protected by a superficial mucus layer, which forms the outermost physical barrier, primarily against infection as well as chemical, enzymatic and mechanical insults.⁴⁹ The composition of the mucus barrier varies between different tissues. Next to antimicrobial peptides such as defensins, cathelicidins, lysozyme, protegrins, collectins and histatins, the major macromolecular mucus components are mucin glycoproteins that are responsible for the viscous, gel-like properties of the mucus layer.⁵⁰ Depending on their site of location and gel-forming properties, up to 20 known mucins can be divided into three subfamilies, i.e. i) secreted, gel-forming mucins; ii) secreted, non-gel forming mucins; and iii) transmembrane, cell-surface mucins.^{49,51} Typically, secreted monomeric mucins cross-link to form extended, homo-oligomeric and viscous networks, whereas their membrane-bound, monomeric counterparts include specific domains that enable their various functions as part of the glycocalyx.⁵¹ In the oral cavity, the mucosa is build up by squamous epithelial cells with underlying salivary glands, which continuously secrete saliva to protect oral and peri-oral tissues as well as to facilitate eating and speech.⁵² Saliva consists of 99% water, but also contains mucin glycoproteins, hormones, vitamins, urea,

several ions and antimicrobial peptides, which form the first line of defense for ingested pathogens.^{53,54}

Measurement of Barrier Functionality *in vitro*

The function of a biological barrier *in vitro* could be determined by the paracellular flux of ions or hydrophilic molecules which are not actively transported transcellularly. This is measured by the transepithelial/transendothelial electrical resistance or by the usage of so-called paracellular marker molecules in tracer flux assays. Histological analysis visualizing tight junction structures using transmission electron microscopy (conventional or freeze fracture) or tight junction proteins via immunofluorescence microscopy are often used to support the functional data.

TEER

The measurement of transepithelial/transendothelial electrical resistance (TEER) is a widely used non-invasive, quantitative method to assess barrier integrity of filter-grown cell models.⁵⁵ TEER reflects the permeability of small ions and is commonly declared as measured ohmic resistance multiplied by growth area of filter-grown models (Ωcm^2). An increased TEER value reflects a tighter paracellular barrier, since less ions can migrate across the cell layer. Changes of TEER were linked to changed expression and/or localization of tight junction proteins such as claudins. In this regard, it is important to mention that different claudins can be either important for the formation of the paracellular barrier or for the set-up of ions pores. For example, following the claudin-nomenclature of Mineta et al.³¹ claudin-1, -3, -4, -5, -6, -8, -9, -11, -14, -18-2 and -19 exhibited preferentially a sealing function and restricted permeability, whereas claudin-2, -7, -10a, -10b, -15, -16, -17 and -21 have been found to form channels in an anion, cation or water specific manner. In this regard, it has to be mentioned that the knowledge for several claudins (-6, -7, -8, -9, -12, -13, -20, -22 to -27) about their function is limited, their effects on epithelial barriers are partly inconsistent and further research has to be accomplished, especially

to understand their role in the complex tight junction networks.^{31,32,56,57}

Thus, not only an increase of barrier-forming claudins, but also a reduction of pore-forming claudins might contribute to an increased TEER value. TEER data are dependent on several parameters such as temperature, used well format, pore-size and porosity of the membranes, membrane materials and the medium used for the measurement (serum content, viscosity, etc.). Consequently, these parameters should be considered when TEER data from different models are compared. In order to determine the TEER of a cell layer, the electrical resistance values of measured blank inserts without cells have to be subtracted from the values obtained with the cell layer, and this difference is multiplied by the surface area. Several different TEER measurement techniques had been developed, their disadvantages and strengths for *in vitro* barrier models have been recently reviewed by Srinivasan *et al.*⁵⁸

Tracer flux assays

In order to assess the paracellular tightness and integrity of barrier-forming epithelia *in vitro*, another possibility is the study of fluorescently or radiolabeled tracer flux across filter-grown cell layers. Frequently used compounds include smaller molecules such as fluorescein, lucifer yellow, mannitol or sucrose, and bigger molecules such as fluorescein isothiocyanate (FITC)-dextrans of various sizes, albumin, IgGs, horseradish peroxidase or inulin. To characterize the transcellular, passive permeability of cell layers lipophilic compounds such as testosterone or diazepam could be used.⁵⁹ These substances should not be substrates of active transport systems and could be used to normalize for cell layers' variabilities in co- or multidose drug transport studies. Results of tracer flux assays are often given as the apparent permeability coefficient (P_{app}) that is defined as the rate of compound accumulation on the opposite of the membrane by time, considering the surface area of the porous membrane as well as the initial drug concentration and the volume of the acceptor chamber.⁶⁰ In contrast to P_{app} , the calculation of the permeability coefficients (PC or P_e) considers the influence of the membrane support for the

transport processes and substrates the permeability across blank membranes without cells in order to obtain the permeability only across the cell layer. This seems to be very relevant for biological barriers with thin basal laminas in the nanometer scale, because the average membrane supports of *in vitro* transwell models are about 10 micrometers thick and thus represent an additional transport barrier.⁶¹

Barrier Studies of the Oral Mucosa

In addition to the culture conditions and the model set-up, the barrier properties of the *in vitro* models of the oral cavity depend on the region of origin and the cell type of the epithelial cells. Therefore, it is essential to know the origin and the type of cells in detail for a proper comparison. To account for this, this chapter begins with a brief overview of the anatomy of the oral cavity followed by the description of the *in vitro* models subdivided in tumor cell derived, primary and immortalized cell lines.

The Oral Cavity – Anatomy

The external anatomical borders of the oral cavity are lips and cheeks. The internal anatomical borders are (i) the anterior pillars of the fauces, (ii) the palate, (iv) the mylohyoid muscle, (iv) the cheeks and (v) the retromandibular region. The oral cavity is covered by three kinds of mucosa: lining, masticatory and specialized mucosa. Lining mucosa is red, consists of non-keratinized stratified squamous epithelium covering the loosely fibrous lamina propria and the submucosa containing fat deposits. This kind of mucosa covers the soft palate, the ventral surface of the tongue, the floor of the mouth, the internal surface of the lips, the cheeks and the alveolar process excluding the masticatory mucosa. Masticatory mucosa is keratinized or parakeratinized and located at the palate, the papilla free dorsal part of the tongue, and the upper part of the alveolar process. In the region of the upper part of the alveolar process and the raphe of the palate, the mucosa is firmly bound to the underlying bone and called gingival mucosa or gingivae, which appears pale pink.

The specialized mucosa is the part where the tongue is dorsally covered by numerous papillae.¹¹

In order to analyze barrier properties of different oral mucosa epithelial subtypes, several authors have applied primary or immortalized keratinocytes and tumor-derived cell lines. Depending on the experimental set-up, epithelial monolayers, multilayers as well as 3D organotypic (co-) cultures have been described as important tools for barrier and permeability studies. Therefore, cells were mainly grown on commercially available filter inserts with varying pore sizes and of different materials like polyethylene terephthalate, polyester or polycarbonate.

Tumor-Derived Cell Lines of the Oral Mucosa

Frequently used cancer cell lines of human oral mucosa and their applications are listed in Table 1, whereas Table 2 provides an overview of immortalized cell lines of oral mucosa. Carcinoma cell lines, together with immortalized and primary cells of oral mucosa that have been used for the investigation of barrier properties are further concretized in Table 3.

For the investigation of oral barrier properties, the human cell line TR146, which originates from a neck node metastasis of buccal carcinoma,⁶² has become a standard model. Thus, filter-grown TR146 cells are stated as a model of human buccal epithelium for more than 20 years.⁶³ The suitability of TR146 cells as an *in vitro* culture model for mechanistic buccal drug delivery, including ionized drugs, and permeability studies has been extensively reported by Jacobsen *et al.* and Nielsen *et al.*^{63–68} TR146 cells are able to form confluent monolayers as well as multilayered, squamous stratified epithelia of approximately 4–7 cell layers and an average thickness of 40 μm after 3 weeks of culture.⁶⁵ TEER and permeation studies of tracers via TR146 epithelial sheets like FITC-dextran with different molecular weights, mannitol or insulin have been extensively studied and are summarized in Table 3. Comparing submerged cultures and cells additionally grown at the air-liquid interface after 10 days of submerged culture, “tightest” permeability barriers with most distinct stratification were formed at day 23, when continuously

Table 1. Human tumor-derived cell lines of oral mucosa.

Cell Line	Studies/Applications/Notes	References ¹
BUCCAL CARCINOMA		
TR146	epithelial barrier studies, model cell line for human buccal epithelium (i.a. drug delivery, trans-epithelial permeability) model cell line for OSCC (i.a. cytotoxicity studies), <i>C. albicans</i> infection studies, 3D organotypic culture (i.a. in commercially available systems of reconstituted oral mucosa, e.g. SkinEthic Laboratories)	62П, 74#, 76, 78, 83, 94–97 barrier/permeability studies see also Table 3 >50 publications (“TR146”)
SqCC/Y1	3D organotypic culture, epigenetic studies, model cell line for malignant buccal carcinoma (i.a. in comparison to normal or immortalized keratinocytes such as SVpgC2a, see Table 3)	98П, 99–102, 103# >40 publications (“SqCC/Y1”)
HO-1-N-1 (Nakata-1; JCRB0831)	wound healing assays/migration, metastasis studies, investigation of retinoic acid (receptors) in OSCC	104П, 105–107#, 108,109 >10 publications (“HO-1-N-1”)
H413 (06092007 SIGMA)	<i>P. gingivalis</i> infection studies, epithelial barrier studies, epigenetic studies, TGFβ studies	110П, 111–114#, 115 barrier/permeability studies see also Table 3 >10 publications (“H413 oral”)
YD-9	1 out of 8 YD oral cancer cell lines (see 116), chemoresistant SCC model cell line, sensitivity to anticancer drugs, cancer-related over-expression studies	116П, 117–120# >10 publications (“YD-9” or “YD9”)
OC3	areca nut-chewing related buccal carcinoma cell line, cytotoxicity studies/tumor suppression	121П, 122,123#, 124,125 >10 publications (“OC3 oral”)
TW2.6	areca nut-chewing and tobacco smoke-related buccal carcinoma cell line, tumor aggressiveness/migration/invasion studies, epigenetic studies	126П, 127#, 128–130 >10 publications (“TW2.6”)
TONGUE CARCINOMA		
CAL27	OSCC model cell line, cancer invasion/migration/metastasis/drug sensitivity studies, ...	131П, recent publications: 132#, 133,134 >100 publications (“Cal27”)
CAL33	OSCC model cell line, cancer invasion/migration/metastasis/drug sensitivity studies, ...	131П, recent publications: 135–137 >40 publications (“Cal33”)
WSU-HN6	cancer cell migration/motility/overexpression studies, drug sensitivity	138П, 139–141 >10 publications (“WSU-HN6”)
H357 (06092004 SIGMA)	OSCC model cell line for several cancer-related studies: drug sensitivity, cell migration, invasion, aggressiveness, ...	110П, recent publications: 142–144 >40 publications (“H357 cancer”)
SCC25 (ATCC® CRL-1628™)	1 out of 6 “SCC” cell lines, weakly invasive (see 145), OSCC model cell line for several cancer-related studies: drug sensitivity, signaling, migration, invasion, ...	145П, recent publications: 133,146,147 ~>300 publications (“SCC25” or “SCC-25”)
D20	moderate dysplastic cell line, 1 out of 16 dysplasias of the oral cavity (see 148), 3D organotypic culture of oral dysplasia	148П, 149–152# > 5 publications (“D20 dysplasia”)
DOK “dysplastic oral keratinocyte”	early and mild/moderate dysplastic cell line, tumor progression/migration studies, 3D organotypic culture of oral dysplasia, analysis of stemcell-associated markers	153П, 150,154–157# >15 publications (“DOK dysplastic”)
OSCC-BD “oral squamous cell carcinoma–B(a)P/DMBA”	established from DOK by B(a)P/DMBA mixture (key carcinogens of tobacco smoke), identification of malignant transformation-related cancer proteins	158П 1 publication (“OSCC-BD”)
HSC-3 (JCRB0623)	OSCC model cell line for several cancer-related studies: drug sensitivity, cell migration, invasion, aggressiveness, cell signaling, stem cell markers ...	159П, recent publications: 160–162 ~>300 publications (“HSC-3 oral” or “HSC3 oral”)
HSC-4 (JCRB0624)	OSCC model cell line for several cancer-related studies: drug sensitivity, cell migration, invasion, aggressiveness, cell signaling, stem cell markers ...	163П, recent publications: 160,164,165 ~>150 publications (“HSC-4 oral” or “HSC4 oral”)
OSC-19	low-grade invasive cell model of epithelial phenotype, metastatic-lesion derived, metastasis studies, epigenetic studies, cytotoxicity studies, drug sensitivity studies, ...	166П, 167–170# >50 publications (“OSC-19 oral” or “OSC19 oral”)
OSC-20	low-grade invasive cell model of epithelial phenotype, metastatic-lesion derived, metastasis studies, cancer stem cell studies, ...	171П, 168,170#,172 >20 publications (“OSC-20 oral” or “OSC20 oral”)
SCCKN	mouse xenograft cell model, cytotoxicity/drug sensitivity studies, ...	173П, 174–176# >20 publications (“SCCKN”)
PE/CA-PJ15	cytotoxicity/drug sensitivity studies, 3D organotypic culture, ...	177П, 156,178–180# >15 publications (“SCCKN”)
YD-8	1 out of 8 YD oral cancer cell lines (see 116), SCC, cytotoxicity/drug sensitivity studies, ...	116П, 181–183# >5 publications (“YD-8” or “YD8”)

(Continued)

Table 1. (Continued).

Cell Line	Studies/Applications/Notes	References ¹
YD-10B	1 out of 8 YD oral cancer cell lines (see ¹¹⁶), SCC, p53-mutant OSCC cell line, cytotoxicity/drug sensitivity studies, ...	¹¹⁶ л, ¹⁸² , ¹⁸³ #, ¹⁸⁴ , ¹⁸⁵ >20 publications ("YD-10B" or "YD10B")
YD-15	1 out of 8 YD oral cancer cell lines (see ¹¹⁶), mucoepidermoid carcinoma, cytotoxicity/drug sensitivity studies, ...	¹¹⁶ л, ¹⁸⁶ – ¹⁸⁸ # >10 publications ("YD-15" or "YD15")
SCC-4 (ATCC® CRL-1624)	OSCC model cell line, metastasis/migration studies, cytotoxicity/drug sensitivity studies, ...	¹⁸⁹ л, recent publications: ¹⁹⁰ , ¹⁹¹ # >100 publications ("SCC-4 oral" or "SCC4 oral")
SCC-9 (ATCC® CRL-1629)	OSCC model cell line, metastasis/migration/invasion studies, overexpression studies, cytotoxicity/drug sensitivity studies, ...	¹⁴⁵ л, recent publications: ¹⁹² , ¹⁹³ >100 publications ("SCC-9 oral" or "SCC9 oral")
SCC-15 (ATCC® CRL-1623)	OSCC model cell line, metastasis/migration/invasion studies, overexpression studies, cytotoxicity/drug sensitivity studies, ...	¹⁸⁹ л, recent publications: ¹⁹⁴ , ¹⁹⁵ # >100 publications ("SCC-15 oral" or "SCC15 oral")
UMSCC2	metastatic SCC cell line, cytotoxicity/drug sensitivity studies, mouse xenograft cell model	¹⁹⁶ – ¹⁹⁸ # >10 publications ("UMSCC2")
SAS	cytotoxicity/drug sensitivity studies, cancer stem cell properties, migration/invasion studies, ...	recent publications: ¹⁹¹ л, ¹⁹⁹ , ²⁰⁰ ~>200 publications ("SAS oral carcinoma")
GINGIVAL CARCINOMA		
Ca9-22	OSCC model cell line, cytotoxicity/drug sensitivity studies, epigenetic studies, cancer-related expression studies, ...	²⁰¹ л, recent publications: ²⁰⁰ , ²⁰² >200 publications ("Ca9-22")
MSCC-1	metastatic-lesion derived, metastasis/migration/invasion studies,	²⁰³ л, ²⁰⁴ 2 publications ("MSCC-1")
KOSC-3	invasion studies, mutational analysis	²⁰⁵ л, ²⁰⁶ – ²⁰⁸ # >5 publications ("KOSC-3" or "KOSC3")
YD-38	1 out of 8 YD oral cancer cell lines (see ¹¹⁶), cytotoxicity/drug sensitivity studies, studies on tumor-associated macrophages	¹¹⁶ л, ¹¹⁷ , ²⁰⁹ , ²¹⁰ # >10 publications ("YD-38" or "YD38")
OEC-M1	Metastasis/migration/invasion studies, cytotoxicity/drug sensitivity studies, cancer-, metastasis- related (over-) expression studies	²¹¹ л, ²¹³ – ²¹⁵ # >40 publications ("OEC-M1 oral" or "OECM1 oral")
CARCINOMA OF THE FLOOR OF THE MOUTH		
KOSC-2	invasion studies, mutational analysis	²⁰⁵ л, ²⁰⁶ , ²⁰⁷ , ²¹⁵ # >5 publications ("KOSC-2" or "KOSC2")
POE-9n	severe dysplastic oral keratinocytes, not immortal but extended culture lifespan, 3D organotypic culture/tissue engineering,	²¹⁶ л, ¹⁵⁰ , ¹⁵⁶ , ²¹⁷ # >5 publications ("POE9n" or "POE-9n")
HO-1-U-1 (Ueda 1; JCRB0828)	metastasis/invasion studies, epithelial barrier studies	⁹⁰ л, ⁹¹ , ⁹³ , ¹⁶⁵ #, ²¹⁸ >15 publications ("HO-1-U-1" or "HO1U1")
H376 (06092005 SIGMA)	nanoparticle transport studies, cancer-related expression studies	¹¹⁰ л, ²¹⁹ – ²²¹ # >10 publications ("H376 oral")
H314 (06092003 SIGMA)	cancer-related expression studies, TGFβ–related studies	¹¹⁰ л, ²²² – ²²⁴ # >5 publications ("H314 oral")
OTHERS (or not specified)		
KB (ATCC CCL-17) <i>epidermoid carcinoma</i> <i>! cross - contaminated with HeLa cells! continued misrepresentation of KB cells as oral cancerphenotype (see ²²⁵)</i>	cancer-related (over-)expression studies, cytotoxicity/drug sensitivity studies, migration/metastasis/invasion studies ...	²²⁶ л, recent publications: ¹²⁰ , ²⁰⁰ , ²²⁷ >300 publications ("KB epidermoid carcinoma oral")
H400 (06092006 Sigma) <i>alveolar process squamous cell carcinoma</i>	cytotoxicity/drug sensitivity studies, 3D organotypic culture	¹¹⁰ л, ²²⁸ – ²³⁰ # >10 publications ("H400 oral")
MEMO <i>oral mucosal melanoma cell line</i>	established from unusual case of oral mucosal melanoma on hard palate and maxillary alveolar ridge	²³¹ л 1 publication, i.e. establishment ("MEMO melanoma")
1483/SCC1483 <i>carcinoma of retromolar trigone region of the oropharynx some stocks genetically identical to UM-SCC1 (see ²³³)</i>	cancer-related expression studies, cytotoxicity/drug sensitivity studies	²³³ л, ²³⁴ – ²³⁶ >10 publications ("1483 retromolar")

(Continued)

Table 1. (Continued).

Cell Line	Studies/Applications/Notes	References ¹
FaDu <i>hypopharyngeal squamous cell carcinoma</i>	migration/invasion studies, cytotoxicity/drug sensitivity studies	^{237Π} ; recent publications: ^{238–240} >80 publications (“FaDu oral”)
BHY <i>squamous cell carcinoma of lower alveolus</i>	cytotoxicity/drug sensitivity studies, cancer-related expression studies	^{241Π} , ^{242–244#} >20 publications (“BHY oral”)
HSC-2 (JCRB0622) <i>SCC of oral cavity</i>	OSCC model cell line, cytotoxicity/drug sensitivity studies, cancer-related (over-) expression studies, metastasis/migration/invasion studies, ...	^{163Π} , recent publications: ^{165,199,245#} >200 publications (“HSC-2 oral” or “HSC2 oral”)
HOC313 <i>OSCC involving the mandibular gingiva and oral floor</i>	high-grade invasive cell model of mesenchymal phenotype, metastatic-lesion derived, cancer progression/metastasis/EMT studies	^{246Π} , ^{170#,247} , ^{248#} >20 publications (“HOC313”)
SCC Cell Line Collections		
PCI cell lines	21 HNSCC cell lines	^{249Π}
JHU cell lines (“John Hopkins University”)	5 SCC cell lines of oral cavity: JHU-011 (larynx), –012 (oral cavity), –013 (oral cavity), –019 (base of tongue), –028 (unknown)	²⁵⁰
73 UM-SCC (“University of Michigan Squamous Cell Carcinoma”) cell lines	73 SCC cell lines of oral cavity	genotyping for all cell lines see ²⁵¹

... latest publication found using respective cell line

Π... publication describing establishment of respective cell line

1) References do not represent a complete list of publications, but list exemplary and/or latest studies. Approximate number of publications should give an impression of how often respective cell lines have been used previously. Search terms are given in parentheses.

abbreviations: HNSCC, head and neck squamous cell carcinoma; OSCC, oral squamous cell carcinoma; SCC, squamous cell carcinoma;

cultured submerged.⁶⁴ Compared to other *in vitro* barrier models of e.g. the gastrointestinal tract or airway epithelium,⁵⁸ TR146 cells form “loose” epithelia with lower TEER values. As summarized in Table 3, TEER is often close to the threshold of 150–200 Ωcm^2 , which are the lowest measurements accepted for drug permeability studies using endothelial cell systems of BBB *in vitro* models.^{69,70} Nonetheless, TR146 cells are a widely accepted model to study oral transmucosal drug delivery, which is considered as an attractive alternative to drug absorption via the gastrointestinal tract.⁷¹ Concretely, TR146 cells are frequently applied to study the effect of permeability enhancers like chitosan,^{72,74} bile salts like sodium glycocholate⁶⁵ or amino acids⁷⁵ on drug transport. TR146 cells were recently used for the evaluation of nanosystems^{76, 77} and for cytotoxicity studies of bioadhesive hydrogels for buccal drug delivery.⁷⁸ Approaches that have shown promising effects in enhancing transport of macromolecules in several *in vitro* and *in vivo* buccal model systems have been extensively reviewed previously.^{79–81} TR146 cells grown at the air-liquid interface have also been used in commercially available 3D models

of human oral mucosa. For example, the reconstituted human oral epithelium from Episkin (Lyon, France) consists of multilayered TR146 cells without submucosal compartments. They have been widely used for *Candida albicans* (*C. albicans*) infection studies.^{82–84}

Another important aspect for epithelial barrier formation are cellular contacts like adherens and tight junctions (TJs). For stratified buccal mucosa it is reported that the paracellular permeability barrier is rather based on membrane coating granules (MCGs) than on TJs.^{85, 86} TEM analysis revealed that TR146 cell sheets do not form TJs.⁶³ In line with this, Teubl *et al.* showed that zona occludens stainings were rare in TR146 cultures.⁸⁷ To our knowledge, the expression of claudin family members has not been studied for the TR146 model.

It also has to be considered that the barrier functionality of oral mucosa *in vivo* is not only made up of integrated epithelial cell sheets. The oral cavity is continuously moistened with saliva, which contains enzymes and the glycoproteins mucins that form an important “external” acellular barrier to mucosal pathogens or nanoparticles.^{49,88} In order to include

Table 2. Immortalized Cell Lines of Oral Mucosa.

Cell Line	Immortalization	Studies/Applications	References ¹
BUCCAL MUCOSA			
SVpgC2a <i>human</i>	SV40T	3D organotypic culture, model cell line for immortalized/transformed buccal keratinocytes, head and neck cancer biomarker study	287II, 99, 253, 100, 282#
NOM9-CT <i>human</i>	Cdk4 + hTERT	effect of curcumin treatment	283III#○
IMOK <i>mouse</i> buccal and palatal mucosa	spontaneous	first cell line to recapitulate mouse oral epithelium differentiation	284)II, 285# ○
foec (clonal cell lines 1–8) <i>mouse</i>	p53-deficient mouse	foec-6, –8: 3D organotypic culture, foec-2, –3, –5, –6, –7, and –8: preparation of bioengineered tooth germ	286III# ○
GINGIVA			
HMK <i>human</i>	spontaneous	3D organotypic culture, HPV/HSV infection studies	287II, 288, 289, 290, 291#
IHGK <i>human</i>	HPV16 E6/E7	normal keratinocytes control cell line for cancer studies, 3D organotypic culture, nicotine studies	292II 293, 294, 295, 296#
MOE (1a and 1b) <i>human</i>	MOE1a: mutant Cdk4, Cyclin D1, hTERT, dominant-negative p53mutant MOE1b: mutant Cdk4, Cyclin D1, hTERT	immortalization process without viral oncogenes	297II#○
GE1 <i>mouse</i>	SV40T	epithelial barrier studies, gingival gene expression studies	257II, 260, 258, 259, 298, 299)#
TIGK <i>human</i>	bmi1/hTERT	bacterial infection studies (mainly <i>P.gingivalis</i>)	300II, 301, 302, 303, 304#
HGEK-16 <i>human</i>	HPV16 E6/E7	3D organotypic culture	305II#○
NDUSD <i>human</i>	SV40T	cytological and cytogenetic characterization	306II#○
OKG4/bmi1/TERT <i>human</i>	bmi1/TERT	3D organotypic culture	216II, 296#
MCNR 3B11 = Gie-No3B11 <i>human</i>	HPV16 E6/E7	epithelial barrier studies, bacterial infection studies (<i>P.gingivalis</i>)	254II, 255, 256#○
OBA-9 <i>human</i>	SV40T	bacterial infection studies	307II, 308, 309, 310, 311#
NOK-SI <i>human</i>	spontaneous	epithelial stem cell functions, wound healing/migration, normal keratinocyte control cell line in cancer and overexpression studies, epigenetics ...	312II, 313, 314, 315, 316#
FLOOR OF THE MOUTH			
OKF-6/TERT2 <i>human</i>	hTERT	3D organotypic culture (oral mucosa equivalents, periodontal biofilm model, bone-oral mucosa model), stemcell-associated marker expression, infection studies (bacteria, <i>C.albicans</i>), toxicological studies ...	216II, 281, 317, 318, 319, 320, 156, 321, 322, 323#
LABIAL VESTIBULE			
GMSM-K <i>human</i>	SV40T	bacterial infection studies, model cell line for normal keratinocytes	324II, 325, 326, 327#○
TONGUE			
ROE2 <i>rat</i>	SV40T	toxicological studies of fluoride	328II, 329#○

... latest publication found using respective cell line

○ ... complete list of publications using respective cell line is given

II... publication describing establishment of respective cell line

1 references do not represent a complete list of publications, but list exemplary and/or latest studies; unless marked with ○

abbreviations: Cdk4, cyclin – dependent kinase 4; HPV16 E6/E7, human papillomavirus 16 E6/E7 proteins; hTERT, human telomerase reverse transcriptase; SV40T, simian virus 40 T antigen

Table 3. Oral Mucosa Cell Models used for *In vitro* Barrier Studies.

Cell Line	Cell Culture Medium	Model Set – Up (permeability assays)	Studied Barrier Properties	References
tumor-derived TR146 <i>human buccal carcinoma</i>	DMEM + 10% FCS + 50 µg/ml gentamicin + 0.2 µg/ml p- hydroxybenzoic acid n-butyl ester	polyethylene terephthalate filters, Becton Dickinson, 1.6×10^6 pores/cm ² , 0.45 µm pore size, 4.6 cm ² growth area, 2.4×10^4 cells/cm ² ; media change: 3x/week	-TEER^A: max. TEER at d30: 55–120 Ωcm ² (inter-passage variation) -tracer flux: mannitol (hydrophilic), min. P_{app} at d30: $\sim 4 \times 10^{-6}$ cm/s; testosterone (lipophilic), P_{app} independent of d: $\sim 2 \times 10^{-5}$ cm/s -TEM: intermediate filaments, microvilli-like processes, no TJs, membrane coating granules, absence of complete keratinization	63
		12-well polyethylene terephthalate filters, Becton Dickinson, 0.4 µm pore size, 0.9 cm ² growth area, 2.1×10^4 cells/filter	-TEER^A: 339 ± 89 Ωcm ² (d28-d30) -tracer flux: ³ H mannitol, FITC-dextran (4 kDa, 10 kDa, 20 kDa); enhancement of permeability by chitosan glutamate; e.g. 4 kDa FITC-dextran: $P_c = 7.85 \pm 2.22$ (x10 ⁷) cm/s increased by 20 µg/ml chitosan to $P_c = 22.52 \pm 6.60$ (x10 ⁷) cm/s; 10 kDa FITC-dextran: $P_c = 2.95 \pm 1.18$ (x10 ⁷) cm/s increased by 20 µg/ml chitosan to $P_c = 5.32 \pm 0.44$ (x10 ⁷) cm/s (more values see Table II in ²⁸⁴)	73
	DMEM + 10% FCS + 3.7 mg/ml NaHCO ₃ + 50 µg/ml gentamicin + 0.2 µg/ml p- hydroxybenzoic acid n-butyl	polyethylene terephthalate filters, Becton Dickinson, 1.6×10^6 pores/cm ² , 0.40 µm pore size, 4.2 cm ² growth area, 2.4×10^4 cells/cm ²	-TEER^A: max. TEER at d23, submerged culture: 102 ± 5 Ωcm ² -tracer flux: ¹⁴ C mannitol, min. P_{app} at d23, submerged culture: $4.08 \pm 0.15 \times 10^{-6}$ cm/s	64
	DMEM + 10% FCS + 100 IU/ml penicillin + 100 µg/ml streptomycin	polyethylene terephthalate filters, Becton Dickinson, 0.40 µm pore size, 4.2 cm ² growth area, 2.4×10^4 cells/cm ²	-TEER^A: 154 ± 13 Ωcm ² (~ d21), decreased by 10 mM GC treatment: 92 ± 49 Ωcm ² -tracer flux: FITC-dextran (4–40 kDa): decreasing P_{app} with increasing M_w 0.65 ± 0.055x10 ⁻⁸ cm/s to 44 ± 7.5x10 ⁻⁸ cm/s;	65
	DMEM + 10% FBS + 200 µM L-glutamine + 100 IU/ml penicillin + 100 µg/ml streptomycin	12 well polyethylene terephthalate filters, Becton Dickinson, 0.4 µm pore size, 0.9 cm ² growth area, 2.2×10^4 cells/cm ²	-TEER^A: 151 ± 38 Ωcm ² (d27-d29), decreased by chitosan treatment (up to 20 mg/ml) treatment (up to 20 mg/ml) -tracer flux: ¹⁴ C mannitol, P_{app} : $3.79 \pm 0.68 \times 10^{-6}$ cm/s, increased by chitosan (NIPAAm-co-MAA), HIM-HEC, HM-EHEC) on cell permeability;	72
			-TEER^A: significant decrease only by chitosan (d27-d29), but reduced cell viability -tracer flux: ¹⁴ C mannitol: significant increase of P_{app} only by chitosan (d27-d29), but reduced cell viability	74

(Continued)



Table 3. (Continued).

Cell Line	Cell Culture Medium	Model Set – Up (permeability assays)	Studied Barrier Properties	References
		12 well PC filters, Corning Costar, 3.0 µm pore size, 1.131 cm ² growth area, 2.4x10 ⁴ cells/cm ² polyethylene terephthalate filters, Becton Dickinson, 0.4 µm pore size, 0.9 cm ² growth area	<p>-TEER^A: 50.02 ± 2.87 Ωcm² (d27-d28)</p> <p>-transport studies of polystyrene nanoparticles using an advanced TR146 model including a mucus layer</p>	87
	DMEM + 10% FCS + 90 IU/penicillin + 90 µg/ml streptomycin	12 well PET filters, Appletonwoods, 2.4x10 ⁴ cells/cm ² ; media change: every 2–3 days	<p>-TEER^A: 36.4 ± 7.6 Ωcm² (d28-d30); 50% decrease by ~ 12 mM GC treatment</p> <p>-tracer flux: ³H mannitol, P_{app}: 3.3 ± 0.4x10⁻⁶ cm/s, increased to 6.4 ± 0.1x10⁻⁶ cm/s by ~ 12 mM GC treatment</p>	330
	Ham's F-12 + 10% FCS + 2 mM glutamine + 100 IU penicillin/ streptomycin + 10 µg gentamicin		<p>-TEER^A: ~ 200 Ωcm² (d30); no significant changes by lysine (10 µg/ml), histidine (10 µg/ml), glutamic acid (100 µg/ml, 200 µg/ml) and aspartic acid (200 µg/ml) treatment</p> <p>-transport studies: insulin, max. permeation: 4.07 ± 0.82% (4h); significant enhancement of insulin permeation by lysine (10 µg/ml), histidine (10 µg/ml), glutamic acid (100 µg/ml, 200 µg/ml), aspartic acid (200 µg/ml) treatment</p>	75
HO-1-u-1 (Ueda-1) human SCC of the floor of the mouth	DMEM-F12 (1:1) + 10% FCS + 50 µg/ml gentamicin + 100 IU/ml penicillin + 100 µg/ml streptomycin	6 well polyethylene terephthalate inserts, Becton Dickinson, 0.45 µm pore size; media change: 3-4x/week	<p>-TEER^A: time-course (d8-d30): continuous increase from 71.4 ± 9.8 Ωcm² to a maximum of 326.3 ± 41.3 Ωcm² (d17), then slowly decrease to 219.1 ± 28.8 Ωcm² (d30)</p> <p>-tracer flux: ¹⁴C mannitol (hydrophilic), P_{app}: decrease from 3.64 ± 0.28 × 10⁻⁶ cm/s (d15) to 2.04 ± 0.17 × 10⁻⁶ cm/s (d26), then slightly increase to 2.42 ± 0.29 × 10⁻⁶ cm/s (d29); ³H testosterone (lipophilic), P_{app} no significant change until d29, ~ 5x10⁻⁶ cm/s; 8 different β-blockers (compounds involving passive diffusion), P_{app}: range from 2.89 ± 0.17 × 10⁻⁶ cm/s (atenolol) to 6.37 ± 0.37 × 10⁻⁶ cm/s (alprenolol) (d2)</p> <p>-TEM: polarized structure, 2–3 cell layers, short microvilli-like processes, desmosomes, no TJs (d23)</p>	91
		6 well polyethylene terephthalate inserts, Becton Dickinson, 0.45 µm pore size, 1.5x10 ⁵ cells/well; media change: 3-4x/week	<p>-TEER^A: no significant differences at various pH (3.5–10), e.g. 175.4 ± 2.5 Ωcm² at pH 3.5, 167.5 ± 9.2 Ωcm² at pH 10</p> <p>-tracer flux: ¹⁴C mannitol, ³H testosterone (neutral markers), P_{app}: independent of solution pH, e.g. ¹⁴C mannitol with 1.92 ± 0.18x10⁻⁶ cm/s at pH 3.5; 1.63 ± 0.14x10⁻⁶ cm/s at pH 10; β-blockers [aterolol (hydrophilic), metoprolol (lipophilic), propranolol (lipophilic)], several P_{app} at different osmolarities and GDC concentrations</p>	93

(Continued)

Table 3. (Continued).

Cell Line	Cell Culture Medium	Model Set – Up (permeability assays)	Studied Barrier Properties	References
GE-1 <i>mouse gingival keratinocytes, temperature-sensitive SV40T immortalization</i>	SFM101 + 1% FCS + 10 ng/ml EGF		<p>-TJ/AJ expression: IF: Cldn1^{pos} (cellular walls), Cldn4^{pos} (cellular walls of medial layers), Cldn5^{neg}, ZO-1^{mod} + RA: Cldn1^{pos} (cytoplasm), Cldn4^{pos} (cellular walls), Cldn5^{pos}, ZO-1^{pos} PCR: Cldn1, Cldn4, Cldn5, Occ, ZO-1 + RA: increased expression of Cldn4, Occ, ZO-1 (n.s.); decreased expression of Cldn1, Cldn5; -gap junction expression: IF: Cx26^{pos}, Cx31.1^{pos}, Cx32^{pos}, Cx43^{pos} PCR: Cx26, Cx30.3, Cx31.1, Cx32, Cx43 + RA treatment: reduced expression of Cx31.1 and Cx32 -TEM: stratified epithelium, desmosomes, hemidesmosomes, anchoring tonofilaments; + RA: thinner cell layer, loss of tonofibrils, less and shorter desmosomes, complete loss of hemidesmosomes -anchoring junctional molecules expression: IF: desmosomes: K13^{pos}, K4^{pos}, desmoglein 1^{pos} + RA: All decreased PCR: desmoglein 1, desmocollin 1, K13, K14, BPAG1, BPAG2, plectin, laminin 5 + RA: decreased expression of desmoglein 1, desmocollin 1, K13, K14, BPAG1; increased expression of plectin; no changes for BPAG2 and laminin 5</p>	258
primary human gingival keratinocytes	DMEM + 15% FCS	24 well collagen® filter inserts, Costar, 4 × 10 ⁵ cells/insert	<p>-TEER^A: 374 Ωcm² (d5), decrease to 120 Ωcm² (d13) -TEM: tight junctions, some desmosomes, no gap junctions</p>	265
	KGM	12 mm Transwell® PC filter inserts, Corning, 0.4 μm pore size, 5 × 10 ⁴ cells/insert	<p>-TEER^A: ~ 100 Ωcm² (~ d3) -TJ/AJ expression: IF: poor detection of Cldn1 (data not shown), no formation of TJs PCR: increased expression of E-cad, β-cat and β-actin by bacterial toxin Cdt (in majority of examined donors)</p>	261
human gingival keratinocytes	KGM	0.40 μM polyethylenetetraphthalate track-etched membranes, BD Biosystems	<p>-TEER^A: 176–208 Ωcm² (independent biopsy samples) -TJ/AJ expression: no expression of ZO proteins (data not shown)</p>	294

(Continued)



Table 3. (Continued).

Cell Line	Cell Culture Medium	Model Set – Up (permeability assays)	Studied Barrier Properties	References
human soft palate keratinocytes	CnT-30 corneal epithelium medium + 1mM CaCl ₂ after 1 day of submerged culture, 6 days airlift in: 1) CnT-30 corneal epithelium medium 2) CnT-30 corneal epithelium medium + 10 ng/ml EGF 3) CnT-30 corneal epithelium medium + conditioned medium from human foreskin fibroblasts 4) CnT-30 corneal epithelium medium + conditioned medium from human foreskin fibroblasts + 10 ng/ml EGF	mouse collagen IV-coated filter inserts, BD Bioscience, 1 µm pores; media change: every day or every 2–3 days	-TEER ^A : medium 1) 2379 ± 1167 Ωcm ² medium 2) 2205 ± 1200 Ωcm ² medium 3) 2007 ± 1119 Ωcm ² medium 4) 1610 ± 439 Ωcm ² (all d13-d17) -TJ/AJ expression: indirect IF: ZO-1 ^{pos} , OccC ^{pos} (medium 1)	267,332
human gingival keratinocytes (EpiGingival™ 3D model, MatTek)	KGM + 0.05 mM CaCl ₂ + 200 mM L-glutamine	24 well plate format	-TJ/AJ expression: PCR: mRNA expression of 62 genes (TJs, AJs, gap junctions; see Table 1 of publication 297)	266

d ... days in culture

Δ ... TEER readings from filters without cells were subtracted from values obtained with filters and seeded cells
 abbreviations: AJ, adherens junction; AM – pectin, amidated pectin; β-cat, β-catenin; CK, cytokeratin; Cldn, claudin; DMEM, Dulbecco's Modified Eagle Medium; E-cad, E – cadherin; EGF, epidermal growth factor; FCS, fetal calf serum; GC, sodium glycocholate; GDC, sodium glycodeoxycholate; HM-EHE, hydrophobically modified ethyl hydroxyethyl cellulose; HM-HEC, hydrophobically modified hydroxyethyl cellulose; HM-pectin, highmethoxylated pectin; hTERT, human telomerase reverse transcriptase; IF, immunofluorescence; JAM-A, junctional adhesion molecule A; LM-pectin, low-methoxylated pectin; MUC, mucin; Occ, occludin; p(NIPAAm-co-MAA, poly(N-isopropylacrylamide-co-methacrylic acid); P_{app}, apparent permeability coefficient; P_c, cellular permeability coefficient; PC, polycarbonate; PET, polyester; SCC, squamous cell carcinoma; TEER, transepithelial electrical resistance; TEM, transmission electron microscopy; TJ, tight junction; WB, Western Blot; ZO, zonula occludens.

mucus as a penetration barrier, an advanced buccal *in vitro* model combining TR146 cells with an adherent mucus layer has been developed.⁸⁷

Due to the carcinogenic nature of TR146, the usage of those cells has shown some limitations. In comparison to normal oral keratinocytes, TR146 based 3D models differ from fully differentiated oral epithelium in terms of histology and differentiation marker expression.⁸⁹ Furthermore, mannitol and testosterone passed the TR146 model ten times faster than human mucosa.⁶⁸ This highlights the fact that a single cell line cannot mimic the complexity of oral tissue *in vitro*.

Another oral mucosa tumor cell line that has been studied for its barrier properties is HO-1-u-1. In more details, HO-1-u-1 (also referred to as “Ueda 1”) is a human tumor cell line derived from a squamous cell carcinoma of the floor of the mouth.⁹⁰ In comparison to buccal mucosa, which is 500–800 μm thick, sublingual mucosa is 190 μm thin, highly vascularized and therefore an attractive target for drug delivery.⁹¹ A well-known example for sublingual drug administration is the treatment of acute angina attacks with nitroglycerin, which is pharmacologically active within 1–2 minutes.⁹² Another advantage of drug delivery via the oral mucosa in general is the circumvention of enzymatic drug degradation in the gut and the liver. In order to analyze sublingual drug delivery, Wang *et al.* presented the HO-1-u-1 cell line as an *in vitro* model for screening of sublingual drug permeation involving passive diffusion.^{91,93} Filter-grown HO-1-u-1 formed stratified, polarized and epithelia-like structures, but were devoid of TJs as characterized by TEM analysis. P_{app} values of β -blockers using the HO-1-u-1 cell model correlated well to those of porcine sublingual mucosa, but measured values were much lower in the cell model, which the authors explained by the loose intercellular structure of HO-1-u-1 layers compared to sublingual tissue.⁹¹ Further evaluation of the HO-1-u-1 model revealed that pH changes are an effective approach to enhance the permeation of β -blockers.⁹³ However, in summary the currently developed *in vitro* models based on

tumor derived cell lines poorly recapitulate barrier properties of the oral mucosa epithelia *in vivo*.

Primary Cells and Immortalized Cell Lines of Oral Mucosa

In contrast to tumor-derived cell lines, the use of primary and immortalized keratinocytes for barrier studies more closely mimics native oral mucosa *in vivo*. In order to circumvent senescence of oral primary keratinocytes, they have been immortalized using different approaches, most frequently including a) silencing of tumor suppressor genes like p53 or KRAS; b) infection with viral oncogenes like HPV-16 E6/E7 or SV40T; or c) telomerase reverse transcriptase (TERT) expression.²⁵² Another possibility is a spontaneous immortalization process where often unknown genetic alterations lead to circumvention of senescence. However, all approaches introduce several molecular changes to the cells, including alterations in DNA, mRNA and miRNA profiles, as characterized recently by Dickman *et al.* for a panel of normal and dysplastic oral cell lines.²⁵² Consequently, immortalized cells can acquire cancer-like features and resemble dysplastic cell lines as described for SV40T-immortalized buccal SVpgC2a cells, which differ from primary keratinocytes in terms of keratin expression, proliferation, apoptosis or responsiveness to serum.²⁵³

Immortalized Cell Lines

A list of immortalized cell lines that have been established from different compartments of the oral mucosa and their primary applications are given in Table 2. Analysis of monocultures revealed that immortalized keratinocytes can show functional characteristics of the epithelial barrier. Gröger *et al.* established immortalized human gingival keratinocyte cell lines with cytokeratin expression patterns comparable to that of primary gingival keratinocytes. Cells formed multi-layered structures, were able to develop TEER and showed expression of claudin-1, claudin-2 and occludin.^{254–256} One of those cell lines, namely Gie-No3B11, was used to study the influence

of retinoic acid (RA) on human gingival epithelial barriers, showing increased TEER, increased claudin-4 and occludin expression, while ZO-1 was downregulated by RA treatment.²⁵⁶ The effect of RA on cell junctions of the gingival epithelium was also studied using the immortalized gingival cell line GE1, which was established from transgenic mice harboring a temperature-sensitive SV40T gene.²⁵⁷ GE1 cells form multilayered structures that are connected by desmosomes.²⁵⁷ Studies by Hatakeyama *et al.* revealed that RA treatment a) altered TJ expression of claudin-1, claudin-4, occludin and ZO-1²⁵⁸; b) decreased the expression of connexin gap junction Cx31.1²⁵⁹ and c) induced downregulation of desmosomes and loss of hemidesmosomes.²⁶⁰

Primary Cells

Formation of oral epithelial barriers by primary cells has also been analyzed. Bacterial infections and their effects on barrier integrity are main foci of several studies, mainly using primary gingival keratinocytes.^{255, 261–263} *P. gingivalis* has been previously described to degrade epithelial cell-cell junctions in Madin-Darby canine kidney (MDCK) cells.²⁶⁴ The occurrence of TJs in gingival tissue has been reported contrarily. Meyle *et al.* identified TJs for cultured primary keratinocytes and gingival biopsies by TEM analysis.²⁶⁵ On the other hand, Damek-Poprawa *et al.* could not detect claudin-1 expression *in vitro*, but did not test for other TJ protein members.²⁶¹ The same study also revealed that the bacterial toxin Cdt induces changes in the distribution and expression of adherens junction components, highlighting that barrier function could also be a consequence of adherens junction stability. The mRNA expression of 62 genes encoding for TJs, gap junctions and adherens junctions was concretized by Belibasakis *et al.* investigated using multilayered gingival epithelial cultures, concretely the commercially available EpiGingivalTM model from MatTek.²⁶⁶ Further studies that analyzed oral mucosa epithelial barriers using primary cells include a multilayered, serum- and feeder-free oral mucosa model of primary cells originating from human soft palate that express TJ proteins

ZO-1 and occludin. Furthermore, Ilmarinen and co-workers reported high TEER values for this model, ranging from 1600–2400 Ωcm^2 , depending on culture medium supplements.²⁶⁷ Compared to other studies with TEER values ranging from approximately 25 Ωcm^2 for human cultivated oral mucosal epithelial sheets²⁶⁸ to 140 Ωcm^2 for human primary gingival primary cells,²⁶⁹ very high TEER values presented by Ilmarinen *et al.* are probably a result of strong stratification.

Tissue-Engineering/Organotypic Cultures

Since cultures of one cell type do not mimic the anatomical complexity of oral mucosa with different infiltrated cell types, blood vessels and submucosal compartments, organotypic co-cultures have been developed. Although a huge variety of set-ups exists, the “basic” components of most 3D *in vitro* oral mucosal systems are stratified, epithelial cell sheets, which are formed onto scaffold-embedded fibroblasts, mimicking submucosal compartments. In oral and maxillofacial surgery, the main objective is the development of biocompatible oral mucosa equivalents as suitable graft materials. Extensive research is done on models for clinical applications such as burn treatment,²⁷⁰ ocular surface reconstruction^{271, 272} or substitution urethroplasty.^{273, 274} Oral mucosa engineering in terms of advantages and disadvantages of different experimental set-ups, cell sources, scaffolds and applications for oral mucosa engineering has been extensively reviewed previously.^{275–278}

To our knowledge, complex full – thickness oral mucosa 3D models, such as approaches including Langerhans cells²⁷⁹ or endothelial cells,²⁸⁰ have not been characterized for their barrier functionality *in vitro*. As described previously, multilayered TR146 cultures are frequently applied for transbuccal drug delivery analyses, although they do not represent a fully differentiated oral epithelium.⁸⁹ As TR146 are derived from buccal carcinoma, 3D models using immortalized oral keratinocytes could be applied in the future to circumvent the limited life-span of primary cells and to enhance the reproducibility of the test model. A widely used immortalized human oral keratinocyte cell line is OKF6/TERT2, which originates from the

Table 4. SALIVARY GLAND EPITHELIAL CELL LINES, This table summarizes cell models that have been used for the study of epithelial barrier properties of salivary glands.

Cell Line	Source	Cell Culture Medium	Characterization (ductal/acinar)	Model Set-Up (permeability assays)	Studied Barrier Properties	References
tumor-derived						
HSG# <i>human</i>	neoplastic submandibular gland intercalated duct epithelium	DMEM/F-12 (1:1) ¹ + 10% FCS + 100 U/ml penicillin + 100 µg/ml streptomycin + 2.5 µg/ml amphotericin B ²	n.a. -non-coated: IF (d5): CK ^{neg} , VIM ^{mod} (88%), αSMA ^{neg} , αAMY ^{neg} , AQP5 ^{neg} , MUC1 ^{neg} -MG-coated: IF (d5): CK ^{pos} , VIM ^{mod} (61%), αSMA ^{neg} , αAMY ^{pos} , AQP5 ^{pos} , MUC1 ^{mod(30%)}	24 mm ³ Transwell PC filter, Corning Costar, 1 × 10 ⁶ cells/well 24 mm Transwell-Clear PET filter, non-coated or MG-coated (f.c. 2 mg/ml, BD Biosciences), 5 × 10 ⁴ cells/cm ²	-TEER^A: 0.50 Ωcm ² (time-course, d0-d5) ⁴ -TJ/AJ expression: IF: ZO-1 ^{neg} , Occ ^{neg} , Cldn1 ^{neg} , Cldn2 ^{neg} , β-cat ^{pos} -TEER^A: -non-coated: 2.1, 3 Ωcm ² (d1, d3, d7) -MG-coated: 401, 417, 332 Ωcm ² (d1, d3, d7) -TJ/AJ expression: IF (d5): -non-coated: Cldn1 ^{neg} , Cldn2 ^{neg} , Cldn3 ^{neg} , Cldn4 ^{neg} , Occ ^{neg} , JAM-A ^{neg} , ZO-1 ^{neg} -MG-coated: Cldn1 ^{pos} , Cldn2 ^{pos} , Cldn3 ^{pos} , Cldn4 ^{pos} , Occ ^{pos} , JAM-A ^{pos} , ZO-1 ^{pos} PCR (d3): -non-coated: Cldn1, Cldn2 -MG-coated: Cldn1, Cldn2 -TEM: -non-coated: small secretory granules, no Golgi apparatus, no rER, no microvilli -MG-coated: secretory-like granules, Golgi saccules, rER, TJs, no basal lamina	346 347
CSG 120/7 <i>mouse</i>	submandibular gland carcinoma	DMEM + 10% FCS + 200 U/ml penicillin + 200 U/ml streptomycin	n.a.	12 mm Transwell filters, 0.4 µm pore size, Costar	-TEER^A: e.g. ~ 250 Ωcm ² (d2), 2350 ± 290 Ωcm ² (d14) (time-course, d0-d14, measured every 2 days) -TJ/AJ expression: IF (d7): Occ ^{pos} , ZO-1 ^{pos} , ZO-2 ^{pos} , JAM-A ^{pos} , E-cad ^{pos} , β-cat ^{pos} -tracer flux: 4 kDa FITC-dextran (0.62 ± 0.39 ng/ml, d14)	357
immortalized						
HSDEC <i>human</i>	-submandibular gland ductal epithelium -hTERT immortalization	BEEM + BEGM Single-Quots (Lonza) + 100 U/ml penicillin + 100 µg/ml streptomycin + 2.5 µg/ml amphotericin B	n.a. IF ⁶ : CK7 ^{pos} , VIM ^{neg}	12 mm Transwell PC filters, 0.4 µm pore size, Millipore 12 mm Transwell filters, 0.4 µm pore size, Corning	-TEER^A: ~ 1700 Ωcm ² (d5); + 100 ng/ml TNFγ: ~ 4000 Ωcm ² ; + 100 ng/ml TGFβ: ~ 100 Ωcm ² -TJ/AJ expression: IF: Cldn4 ^{pos} , Cldn7 ^{pos} , Occ ^{pos} , JAM-A ^{pos} + 100 ng/ml TNFγ: increased Cldn7 expression (WB, PCR), strong expression of Occ (IF); + 100 ng/ml TGFβ: lower expression of Occ at cell borders (IF)	358 7

(Continued)



Table 4. (Continued).

Cell Line	Source	Cell Culture Medium	Characterization (ductal/acinar)	Model Set-Up (permeability assays)	Studied Barrier Properties	References
SMIE <i>rat</i>	-submandibular gland -adenovirus 12S ETA gene product immortalization	DMEM + 10% FCS + 100 U/ml penicillin + 100 µg/ml streptomycin	n.a.	24 mm Transwell filters, 0.4 µm pore size, Corning Costar, 10 ⁵ cells/cm ²	<p>-TEER^A: 058 Ωcm² (time-course, d4-d7); overexpression of GFP-Cldn4: ~ 40 Ωcm² (3d after plating, i.e. 2d after transfection); ~ 80 Ωcm² (4d after plating, i.e. 3 days after transfection)</p> <p>-TJ/AJ expression: IF (d4): ZO-1^{pos}, Occ^{pos}, Cldn3^{pos}, Cldn4^{neg} WB (d n.i.): E-cad, Occ, Cldn3, Cldn2^{n.d.}, Cldn4^{n.d.}, Cldn6-8^{n.d.}, Cldn10^{n.d.}, Cldn12^{n.d.} PCR (d n.i.): E-cad, Occ, Cldn3⁷, Cldn12, Cldn1^{n.d.}, Cldn2^{n.d.}, Cldn4^{n.d.}, Cldn¹¹, Cldn14^{n.d.}, Cldn20^{n.d.}, Cldn22^{n.d.}, Cldn23^{n.d.}</p> <p>-tracer flux⁸: 4 kDa FITC-dextran (~ 18% paracellular flux of input), 70 kDa FITC-dextran (~ 8% paracellular flux of input); overexpression of GFP-Cldn4: decreased flux of 4 kDa and 70 kDa FITC-dextran (4d after plating, i.e. 3 days after transfection)</p> <p>-TEER^A: ~ 40 Ωcm² (d10), serum-free: < 10 Ωcm² (d10)</p> <p>-TJ/AJ expression: IF (d10): ZO-1^{pos}, Occ^{pos} WB (d10): Cldn3, Occ, Cldn4^{n.d.}</p> <p>-tracer flux: 4 kDa FITC-dextran (~ 15% paracellular flux of empty filter control; serum-free: ~ 75% paracellular flux of control)⁹</p> <p>-TEER^A: ~ 30 Ωcm² (d n.i.) -TJ/AJ expression: IF (d7): ZO-1^{pos}</p>	340
			n.a.	24 mm Transwell types I and III collagen-coated PC inserts, Corning, 0.4 µm pore size, 3 × 10 ⁶ cells/well	<p>-TEER^A: ~ 40 Ωcm² (d10), serum-free: < 10 Ωcm² (d10)</p> <p>-TJ/AJ expression: IF (d10): ZO-1^{pos}, Occ^{pos} WB (d10): Cldn3, Occ, Cldn4^{n.d.}</p> <p>-tracer flux: 4 kDa FITC-dextran (~ 15% paracellular flux of empty filter control; serum-free: ~ 75% paracellular flux of control)⁹</p> <p>-TEER^A: ~ 30 Ωcm² (d n.i.) -TJ/AJ expression: IF (d7): ZO-1^{pos}</p>	359
			n.a.	24.5 mm Transwell types I and III collagen-coated PC filter, Costar, 3 × 10 ⁶ cells/well	<p>-TEER^A: ~ 40 Ωcm² (d10), serum-free: < 10 Ωcm² (d10)</p> <p>-TJ/AJ expression: IF (d10): ZO-1^{pos}, Occ^{pos} WB (d10): Cldn3, Occ, Cldn4^{n.d.}</p> <p>-tracer flux: 4 kDa FITC-dextran (~ 15% paracellular flux of empty filter control; serum-free: ~ 75% paracellular flux of control)⁹</p> <p>-TEER^A: ~ 30 Ωcm² (d n.i.) -TJ/AJ expression: IF (d7): ZO-1^{pos}</p>	360

(Continued)

Table 4. (Continued).

Cell Line	Source	Cell Culture Medium	Characterization (ductal/acinar)	Model Set-Up (permeability assays)	Studied Barrier Properties	References
SMG-C6 <i>rat</i>	-submandibular gland acinar cells -replication defective SV40 immortalization	DMEM/F-12 (1:1) + 2.5% FCS + 5 µg/ml transferrin + 1.1 µmol/l hydrocortisone + 0.1 µmol/l retinoic acid + 2 nmol/l thyronine T3 + 5 µg/ml insulin + 80 ng/ml EGF + 50 µg/ml gentamicin sulfate + 5 mmol/l glutamine + 100 U/ml penicillin + 100 µg/ml streptomycin	WB (d n.i.): CK19 ^{neg}	12 mm Snapwell PC filters, 0.4 µm pore size, Costar, coated with 1.0 µg/cm ² human collagen type I (Becton Dickinson), 2.5x10 ⁵ cells/cm ² 6.5 mm Transwell filters, Corning, 0.4 µm pore size, 3.8x10 ⁵ cells/cm ²	-TEER ^A : 956 ± 84 Ωcm ² (d n.i.) -TEER ^A : 463.69 ± 13.35 Ωcm ² (d6); + TNFα: concentration- + time-dependent decrease, e.g. to ~200 Ωcm ² (50 ng/ml, 48h) -TJ/AJ expression: PCR ± WB (d n.i.): Cldn1, Cldn3, Cldn4, ZO-1, ZO-2, β-cat; + TNFα: concentration- + time-dependent disruption of Cldn3 distribution (WB, IF) -tracer flux: 4 kDa + 40 kDa FITC-dextran (time course 0-48h, start d6) ¹⁰ ; + TNFα: 4 kDa and 40 kDa FITC-dextran flux significantly elevated (24h, 48h) * overexpression, depletion or re-expression of Cldn3 altered the response of TNFα induced paracellular permeability and tight junction contents	345 8
			n.a.	24 well Transwell chambers (0.33 cm ² growth area), 0.4 µm pore size, Costar	-TEER ^A : ~600 Ωcm ² (d6/7) ¹¹ ; no altered TEER by ZO-1, ZO-2, ZO-1/ZO-2 KD; significant drop in TEER by CAP (4-60min), but effect reversed in ZO-1, ZO-2, ZO-1/ZO-2 KD -TJ/AJ expression: PCR ± IF ± WB (d n.i.): ZO-1, ZO-2, ZO-3, Occ, β-cat -tracer flux: 4 kDa FITC-dextran ¹¹ ; 4 kDa FITC-dextran flux significantly increased in ZO-1, ZO-2, ZO-1/ZO-2 KD, CAP significantly increased 4 kDa FITC-dextran flux, no effect in KD cells	361
			n.a.	24 well Transwell chambers (0.33 cm ² growth area), PC filter, Costar, confluent density	-TEER ^A : 516.2 ± 98.62 Ωcm ² (d5-d7); + CAP: concentration- + time-dependent decrease + Occ KD or ERK1/2 KD: significant decrease in TEER -TJ/AJ expression: IF (d n.i.): E-cad ^{pos} , β-cat ^{pos} , Cldn3 ^{pos} PCR (d n.i.): ZO-1, Occ, Cldn1, Cldn3, Cldn4, Cldn2 ⁿ , Cldn5 ^{h,d} . WB: Occ	362

(Continued)



Table 4. (Continued).

Cell Line	Source	Cell Culture Medium	Characterization (ductal/acinar)	Model Set-Up (permeability assays)	Studied Barrier Properties	References
Par-C10 <i>rat</i>	-parotid gland acinar cells -replication defective SV40 immortalization	DMEM-F12 (1:1) + 2.5% FCS + 0.1 µM retinoic acid + 80 ng/ml EGF + 2 nM thyronine T3 + 5 mM glutamine + 0.4 µg/ml hydrocortisone + 5 µg/ml insulin + 5 µg/ml transferrin + 5 ng/ml sodium selenite + 50 µg/ml gentamicin + 8.4 ng/ml cholera toxin	n.a.	24 well Transwell chambers, PC filter (0.33 cm ² growth area), 0.4 µm pore size, Costar	<p>-tracer flux: 4 kDa FITC-dextran, trypan blue¹² + CAP: increased permeability for 4 kDa FITC-dextran and trypan blue</p> <p>-TEER^A: 632.8 ± 107.1 Ωcm² (d7); + Cch: concentration- + time-dependent decrease</p> <p>-TJ/AJ expression: WB (d n.i.): E-cad, Occ, ZO-1, Cldn1, Cldn4 IF (d n.i.): Cldn4^{pos}, Occ^{pos}, ZO-1^{pos}, + Cch: altered distribution of Cldn4 (IF)</p> <p>-tracer flux: 4 kDa + 40 kDa FITC-dextran¹², + Cch: concentration- + time-dependent increase of 4 kDa flux</p> <p>-TEER^A: 592.67 + 29.8 Ωcm² (d n.i.); + AICAR: decreased TEER values by ~ 46% (60min); Ca2+ free medium decreased TEER values by ~ 60% (60min);</p> <p>-TJ/AJ expression: WB ± IF (d n.i.): Occ, ZO-1, Cldn1, Cldn3, Cldn4 + AICAR: altered distribution of Cldn4 (IF)</p> <p>-tracer flux: 4 kDa FITC-dextran¹², + AICAR: increased permeability of 4 kDa FITC-dextran by 81.59% (60min)</p> <p>-TEER^A: 635 ± 36.64 Ωcm² (d5/6/7); time-dependent decrease of TEER: + fAd (~ 60% decrease, 30min), + gAd (~ 60% decrease, 60min), + AICAR (~ 40% decrease, 60min)</p> <p>-TEM: secretory granules, TJ, intermediate junctions, desmosomes, microvilli</p> <p>-TEER^A: ~ 3500 Ωcm² (d4); + TNFα/INFγ: concentration- + time-dependent decrease, e.g. + 10 ng/ml TNFα: ~ 1200 Ωcm² (48h), + 10 ng/ml INFγ: ~ 2000 Ωcm² (48h), + 10 ng/ml TNFα/INFγ: ~ 400 Ωcm² (48h)</p> <p>-TJ/AJ expression: WB (d n.i.): Cldn1, Cldn3, Cldn4, Cldn10, Occ, ZO-1, JAM-A</p> <p>-tracer flux: 1.9 kDa/20Å microperoxidase MP-11, 44 kDa/50–60 Å horseradish peroxidase type VI, 80 kDa/120Å bovine milk lactoperoxidase³, + TNFα, + INFγ, + TNFα/INFγ: increased permeability of microperoxidase MP-11 and horseradish peroxidase type VI</p>	342
			n.a.	24 well Transwell chambers, PC filter, 0.33 cm ² growth area, 0.4 µm pore size, Costar	<p>-TEER^A: 592.67 + 29.8 Ωcm² (d n.i.); + AICAR: decreased TEER values by ~ 46% (60min); Ca2+ free medium decreased TEER values by ~ 60% (60min);</p> <p>-TJ/AJ expression: WB ± IF (d n.i.): Occ, ZO-1, Cldn1, Cldn3, Cldn4 + AICAR: altered distribution of Cldn4 (IF)</p> <p>-tracer flux: 4 kDa FITC-dextran¹², + AICAR: increased permeability of 4 kDa FITC-dextran by 81.59% (60min)</p> <p>-TEER^A: 635 ± 36.64 Ωcm² (d5/6/7); time-dependent decrease of TEER: + fAd (~ 60% decrease, 30min), + gAd (~ 60% decrease, 60min), + AICAR (~ 40% decrease, 60min)</p> <p>-TEM: secretory granules, TJ, intermediate junctions, desmosomes, microvilli</p> <p>-TEER^A: ~ 3500 Ωcm² (d4); + TNFα/INFγ: concentration- + time-dependent decrease, e.g. + 10 ng/ml TNFα: ~ 1200 Ωcm² (48h), + 10 ng/ml INFγ: ~ 2000 Ωcm² (48h), + 10 ng/ml TNFα/INFγ: ~ 400 Ωcm² (48h)</p> <p>-TJ/AJ expression: WB (d n.i.): Cldn1, Cldn3, Cldn4, Cldn10, Occ, ZO-1, JAM-A</p> <p>-tracer flux: 1.9 kDa/20Å microperoxidase MP-11, 44 kDa/50–60 Å horseradish peroxidase type VI, 80 kDa/120Å bovine milk lactoperoxidase³, + TNFα, + INFγ, + TNFα/INFγ: increased permeability of microperoxidase MP-11 and horseradish peroxidase type VI</p>	341
			n.a.	24 well Transwell chambers, PC filter 0.33 cm ² growth area, 0.4 µm pore size, Costar	<p>-TEER^A: 635 ± 36.64 Ωcm² (d5/6/7); time-dependent decrease of TEER: + fAd (~ 60% decrease, 30min), + gAd (~ 60% decrease, 60min), + AICAR (~ 40% decrease, 60min)</p> <p>-TEM: secretory granules, TJ, intermediate junctions, desmosomes, microvilli</p> <p>-TEER^A: ~ 3500 Ωcm² (d4); + TNFα/INFγ: concentration- + time-dependent decrease, e.g. + 10 ng/ml TNFα: ~ 1200 Ωcm² (48h), + 10 ng/ml INFγ: ~ 2000 Ωcm² (48h), + 10 ng/ml TNFα/INFγ: ~ 400 Ωcm² (48h)</p> <p>-TJ/AJ expression: WB (d n.i.): Cldn1, Cldn3, Cldn4, Cldn10, Occ, ZO-1, JAM-A</p> <p>-tracer flux: 1.9 kDa/20Å microperoxidase MP-11, 44 kDa/50–60 Å horseradish peroxidase type VI, 80 kDa/120Å bovine milk lactoperoxidase³, + TNFα, + INFγ, + TNFα/INFγ: increased permeability of microperoxidase MP-11 and horseradish peroxidase type VI</p>	363
			n.a.	12 mm Falcon permeable supports, 0.4 µm pore size, Becton Dickinson, 5 × 10 ⁵ cells/well	<p>-TEER^A: ~ 3500 Ωcm² (d4); + TNFα/INFγ: concentration- + time-dependent decrease, e.g. + 10 ng/ml TNFα: ~ 1200 Ωcm² (48h), + 10 ng/ml INFγ: ~ 2000 Ωcm² (48h), + 10 ng/ml TNFα/INFγ: ~ 400 Ωcm² (48h)</p> <p>-TJ/AJ expression: WB (d n.i.): Cldn1, Cldn3, Cldn4, Cldn10, Occ, ZO-1, JAM-A</p> <p>-tracer flux: 1.9 kDa/20Å microperoxidase MP-11, 44 kDa/50–60 Å horseradish peroxidase type VI, 80 kDa/120Å bovine milk lactoperoxidase³, + TNFα, + INFγ, + TNFα/INFγ: increased permeability of microperoxidase MP-11 and horseradish peroxidase type VI</p>	364
			n.a.	12 mm Falcon permeable supports, 0.4 µm pore size, Becton Dickinson, 5 × 10 ⁵ cells/well	<p>-TEER^A: ~ 3500 Ωcm² (d4); + TNFα/INFγ: concentration- + time-dependent decrease, e.g. + 10 ng/ml TNFα: ~ 1200 Ωcm² (48h), + 10 ng/ml INFγ: ~ 2000 Ωcm² (48h), + 10 ng/ml TNFα/INFγ: ~ 400 Ωcm² (48h)</p> <p>-TJ/AJ expression: WB (d n.i.): Cldn1, Cldn3, Cldn4, Cldn10, Occ, ZO-1, JAM-A</p> <p>-tracer flux: 1.9 kDa/20Å microperoxidase MP-11, 44 kDa/50–60 Å horseradish peroxidase type VI, 80 kDa/120Å bovine milk lactoperoxidase³, + TNFα, + INFγ, + TNFα/INFγ: increased permeability of microperoxidase MP-11 and horseradish peroxidase type VI</p>	9

(Continued)

Table 4. (Continued).

Cell Line	Source	Cell Culture Medium	Characterization (ductal/acinar)	Model Set-Up (permeability assays)	Studied Barrier Properties	References
Par-C5 = Pa-4 <i>rat</i>	-parotid gland acinar cells -replication defective SV40 immortalization	DMEM F-12 (1:1) + 2.5% FCS + 5 µg/ml insulin + 5 µg/ml transferrin + 25 ng/ml EGF + 1.1 µM hydrocortisone + 5 mM glutamate + 60 µg/ml kanamycin monosulfate ¹⁴	n.a.	-Transwell, collagen-coated clear PC filters, 1 cm ² growth area, 0.4 µm pore size, Costar, 10 ⁶ cells/cm ²	-TEM: secretory granules, TJ, intermediate junctions, desmosomes, microvilli -TEER^A: 2000 Ωcm ² (d7) -TJ/AJ expression: IF (d n.i.): Occ ^{pos} , ZO-1 ^{pos} , E-cad ^{pos} WB (d n.i.): Occ, ZO-1, E-cad, Cldn1	364 343
			n.a.	Cleanwell, Costar Corning	-TEER^A: ~ 2000 Ωcm ² (d5) -TJ/AJ expression: IF (d n.i.): β-cat ^{pos} , Occ ^{pos}	344

d ... days in culture, n.a. ... not analyzed, n.i. ... not indicated, n.d. ... not detected, f.c. ... final concentration

... listed as cross-contaminated cell lines (Hela derivatives by ATCC, ECACC)

Δ ... TEER readings from filters without cells were subtracted from values obtained with filters and seeded cells

1) establishment and characterization in different cell culture medium: MEM, 10% FCS, 2 mmol/l L-glutamine^{365,366}

2) different antibiotic/antimycotic substances used: 10 mg/ml gentamicin instead of 2.5 µg/ml amphotericin B³⁴⁷

3) for Transwell inserts, membrane *diameters* are given in mm

4) collagen I/III coating of filters had no effect on TEER

5) CSG WT monolayers used as control cell line, i.e. inulin flux set to 100%

6) for all experiments, cells were used at the second passage, 5 – 7 days after plating

7) Cldn3 main claudin expressed in SMIE cells

8) for FITC-dextran flux, medium was changed to HEPES-buffered saline (10 mM HEPES/NaOH pH 7.4; 1 mM sodium pyruvate, 10 mM glucose, 3 mM CaCl₂, 145 mM NaCl)

9) for FITC-dextran flux, medium was changed to DMEM containing 10 mM HEPES buffer (pH 7.4)

10) WT SMG-C6 monolayers given as "relative paracellular flux"¹¹ = 1

11) TEER and paracellular flux given for scrambled siRNA SMG-C6 control cells, i.e. relative paracellular flux of FITC-dextran set to 1

12) apparent permeability coefficients given as "% of initial value", WT SMG-C6 set to 100%

13) peroxidase activity in cell supernatant given as "absorbance values at 405nm"

14) Li *et al.*³⁴³ used 600 µg/ml G418 instead of kanamycin monosulfate; Quissel *et al.*³⁶⁴ additionally used 8.4 ng/ml cholera toxin

abbreviations: αAMY, α amylase; αSMA, α smooth muscle actin; AICAR, 5-aminoimidazole-4-carboximidobutyl nucleoside (AMPK activator); AJ, adherens junction; AMPK, AMP-activated protein kinase; AQP, aquaporin; β-cat, β-catenin; BEBM, bronchial epithelial basal medium; CAP, capsacin; Cch, carbachol; CK, cytokeratin (panel); Cldn, claudin; DMEM, Dulbecco's Modified Eagle Medium; E-cad, E – cadherin; EGF, epidermal growth factor; fAd, full length adiponectin; FCS, fetal calf serum; gAd, globular adiponectin; hTERT, human telomerase reverse transcriptase; IF, immunofluorescence; JAM-A, junctional adhesion molecule A; MEM, minimum essential media; MG, Matrigel; MUC, mucin; Occ, occludin; PC, polycarbonate; PET, polyester; TEM, transmission electron microscopy; TEER, transepithelial electrical resistance; TJ, tight junction; VIM, vimentin; WB, Western Blot; ZO, zonula occludens;

floor of the mouth. A standardized protocol of OKF6/TERT2 cells cultured on fibroblasts-populated collagen gels, grown at the air-liquid interface, has been published previously.²⁸¹

Barrier Studies of Salivary Glands

In order to be able to assess the data of *in vitro* models of salivary gland epithelia in a proper manner, it is important to know about the diversity, structure, anatomy and cell types of salivary glands. Moreover, to evaluate and develop models which are functionally similar to the *in vivo* epithelium it is crucial to become acquainted with the production and composition of saliva. Therefore, this chapter starts with a brief introduction of the anatomy of salivary glands and saliva's production and composition, before barrier studies using models of the salivary gland epithelia are described in detail.

Salivary Glands – Anatomy

Salivary glands are tubuloacinar exocrine glands with ducts opening into the oral cavity. The glands secrete saliva, which moisten the mucosa, lubricate food for deglutition and works as a solvent for taste and has many more functions. Saliva also contains digestive enzymes such as amylase and antimicrobial agents such as immunoglobulin A, lysozyme and lactoferrin which are secreted by the salivary glands. Saliva seems to have disease preventive properties, as a significant decrease in saliva production can lead to diseases such as periodontal inflammation and dental caries.¹¹

The parotid, submandibular and sublingual glands are the three major paired salivary glands. Numerous other minor salivary glands open into the mouth and are scattered throughout the oral cavity. The parotid gland, the largest of the saliva glands, is situated in front of the external ear and is almost entirely serous. The palpable parotid duct runs superficial of the buccinator muscle and through the cheek to drain into the mouth opposite of the second permanent maxillary molar. The submandibular gland is the size of a walnut and irregular in shape but generally spheroid and is located at the posterior and lower part of the mylohyoid muscle and mostly serous. The sublingual gland is

the smallest of the three major paired salivary glands; it is flat and shaped like an almond. The location is cranial of the mylohyoid muscle and beneath the mouth floor mucosa. The sublingual gland is seromucous but most cells are mucous.¹¹

Salivary glands are separable in numerous lobes, which are composed of smaller lobules containing excretory ducts, blood vessels, lymph vessels, nerve fibers and small ganglia. Each duct has branches beginning with dilated secretory “endpieces”, with which the flow of saliva starts. The endpieces can be either tubular or acinar in shape. Different types endpieces can be dominant in the different salivary glands. In the parotid and submandibular gland, the secretory units are mostly serous acini with a few mucous tubules and acini. In the submandibular glands, the dominant cells are the mucous tubules and acini; a minority of serous cells occur as acini or demilunes.¹¹

Myoepithelial cells are associated with secretory endpieces and have an abundance of actin microfilaments which facilitate contraction; these contractions accelerate the outflow of saliva and contribute to the secretory pressure. Lining cells of the ducts are flat near the secretory endpiece and become more cuboidal in excretion direction. Lining cells function as a conduit for saliva. Together with striated ducts, lining cells may modify the salivary content with regard to electrolytes and immunoglobulin A.¹¹ The striated ducts cells build a low columnar epithelium with eponymous basal striations. The striations are a highly infolded region of the basal plasma membrane. Mitochondria being abundant in these infolded regions, are typical for epithelial cells that actively transport electrolytes. Collecting ducts run between the lobes and transport the saliva to the main duct. In the main duct, the lining cells may vary, they can be pseudostatified columnar, stratified cuboidal or columnar, with a distinct basal layer, and a stratified squamous epithelium near the buccal orification.¹¹

Saliva production and composition

In a lifetime a human produces about 25,000 liters of saliva. The unstimulated saliva secretion is about 15 mL/h, of this the parotid glands secrete 25%, the submandibular glands 60% and

Table 5. Salivary gland primary epithelial cells: This table summarizes primary cell culture techniques that have been used for the study of epithelial barrier properties of salivary glands.

Primary Cells	Cell Culture Medium	Passage used	Max. used	Characterization (ductal/acinar)	Model Set-Up (permeability assays)	Studied Barrier Properties	References
phMSG <i>human minor salivary gland</i>	KGM-high (0.8 nM Ca ²⁺) + BPEs + hEGF + insulin + hydrocortisone + gentamicin + epinephrine + transferrin ¹ serum-free Hepato-STIM + 1% glutamine + 500 U/ml penicillin + 500 µg/ml streptomycin + 12.5 µg/ml fungizone	8–10 (in KGM-low, 0.05 nM Ca ²⁺)		-PCR (d3) ² : ZO-1 ^{high} , CLDN1 ^{high} , AQP5 ^{relhigh} , SLC12A2 ^{relhigh} , CST3 ^{relhigh} , ORAI1 ^{relhigh} , αAMY ^{modest} , ANO1 ^{modest} , KRT19 ^{low} , KLK1 ^{low} -IF (d3): SLC12A2 ^{pos} , CSTE ^{pos} , AQP5 ^{pos} -agonist-induced αAMY secretion and activity	Transwell-COL, collagen-coated PET filter, 0.4 µm pore size, Corning, 20 × 10 ⁴ cells/well	-TER^{A3} : ~ 90–180 Ωcm ² (time-course, d3-d10) -TJ/AJ expression : IF (d3): ZO-1 ^{pos} PCR (d3): E-cad, ZO-1, Cldn1	367
huSMG <i>human submandibular gland</i>		n.i.		-IF (d n.i.): E-cad ^{pos} , Vim ^{neg}	24 mm Transwell-Clear, PET filter, Corning	-TER^A : ~ 250–300 Ωcm ² (d n.i.) -TJ/AJ expression : IF (d n.i.): ZO-1 ^{pos} , Cldn1 ^{pos} , E-cad ^{pos} -TEM : tight junctions, microvilli, no secretory granules	368
huSG <i>human submandibular or parotid gland</i>		3		-PCR (d n.i.): αAMY, AQP5, NKCC1, ENaC, Cldn1 - αAMY secretion: strong secretion on Transwell vs plastic (5022–1682 U/l vs 742–214 U/l) -IF (d n.i.): non-coated: CK ^{pos(85%)} , VIM ^{mod(40%)} , αSMA ^{neg} , αAMY ^{neg} , AQP5 ^{neg} , MUC1 ^{neg} MG-coated: CK ^{pos} , VIM ^{pos} , αSMA ^{neg} , αAMY ^{pos} , AQP5 ^{pos} , MUC1 ^{mod(50%)} -enhanced αAMY secretion in MG-coated set-up	Transwell-Clear, PET filters, FCS-coated, 0.4 µm pore size, 1.12 cm ² growth area, Corning Costar	-TER^A : 622 ± 117 Ωcm ² (d7-d10) ⁴ -TJ/AJ expression : PCR (d n.i.): Cldn1	369 5
huSG <i>human submandibular or parotid gland</i>	serum-free Hepato-STIM + 1% glutamine + 500 U/ml penicillin + 500 µg/ml streptomycin + 12.5 µg/ml fungizone	3			24 mm Transwell-Clear, non-coated or MG-coated (f.c. 2 mg/ml BD Biosciences) PET filters, Corning, 5 × 10 ⁴ cells/cm ²	-TER^A : non-coated: 381, 409, 415 Ωcm ² (d3, d5, d7); MG-coated: 409, 407, 415 Ωcm ² (d3, d5, d7) -TJ/AJ expression : IF (d n.i.): non-coated± MG-coated: Cldn1 ^{pos} , Cldn2 ^{pos} , Cldn3 ^{pos} , Cldn4 ^{pos} , Occl ^{pos} , JAM-A ^{pos} , ZO-1 ^{pos} -TEM : non-coated: TJs, no Golgi apparatus, no rER, no secretory granules, no microvilli MG-coated: TJs, many Golgi saccules, rER, secretory granules	370
PTHSG ⁶ <i>human submandibular gland</i>	Hepato-STIM + 10% FCS + 1% glutamine + 500 U/ml penicillin + 500 µg/ml streptomycin + 12.5 µg/ml fungizone	4		IF (p0): non-coated or BME-coated: αAMY ^{pos} and αAMY ^{neg} clusters, non-coated: some Vim ^{pos} clusters, BME-coated: Vim ^{neg}		-TJ/AJ expression : PCR: describes differential expression of αAMY, Cldn1, Cldn3, KLK and Vim in 13 patients	371

(Continued)



Table 5. (Continued).

Primary Cells	Cell Culture Medium	Max. Passage used	Characterization (ductal/acinar)	Model Set-Up (permeability assays)	Studied Barrier Properties	References
		3	-PCR (d n.i.): α AMY, AQP5, NKCC1, ENaC, Cldn1 - α AMY secretion: strong secretion on Transwell vs plastic (3043–882 U/l vs 568–193 U/l) IF (d n.i.): E-cad ^{pos} , Na/K ATPase ^{pos}	Transwell-Clear, PET filters, FCS-coated, 0.4 μ m pore size, 1.12 cm ² growth area, Corning Costar	-TER^A : $595 \pm 93 \Omega\text{cm}^2$ (d7-d10) ⁴ -TJ/AJ expression : PCR (d n.i.): Cldn1	369
RPG <i>rhesus monkey parotid gland</i>	serum-free Hepato-STIM + 1% glutamine + 500 U/ml penicillin + 500 μ g/ml streptomycin + 12.5 μ g/ml fungizone	4	IF (d n.i.): E-cad ^{pos} , Na/K ATPase ^{pos}	24 mm Transwell-Clear, PET filter, Corning	-TER^A : $\sim 135 \Omega\text{cm}^2$ (d3) -TJ/AJ expression : IF (d n.i.): E-cad ^{pos} , ZO-1 ^{pos} , Cldn1 ^{pos} -restricted paracellular fluid movement (2.0 μ l/cm ² vs. 6.5 μ l/cm ² in HSG)	372
ASGE <i>BALB/c mouse submandibular gland</i>	DMEM-F12 + 2 mM glutamine + 10 ng/ml EGF + 5 μ g/ml insulin + 5 μ g/ml transferrin + 100 U/ml penicillin + 100 U/ml streptomycin + 0.25 μ g/ml amphoteri ^c + 2 nM triiodothyronine T3 + 0.4 μ g/ml hydrocortisone + 0.18 mM adenine + 100 nM cholera toxin	5	IF (d n.i.): CK ^{pos} , VIM ^{neg} (ASGEs on feeder layer of irradiated, VIM ^{pos} NIH fibroblasts)	24 mm Transwell, PC filters, Corning Costar, 1×10^6 cells/well	-TER^A : $\sim 150 \Omega\text{cm}^2$ (d5) -TEM : desmosomes, TJs, microvilli, secretory granules (ASGEs on feeder layer of irradiated NIH 3T3 fibroblasts)	373

d ... days in culture, n.a. ... not analyzed, n.i. ... not indicated, n.d. ... not detected, f.c. ... final concentration

Δ ... TEER readings from filters without cells were subtracted from values obtained with filters and seeded cells

1 Jang *et al.*³⁶⁷ tested 6 differently supplemented growth media (no concrete supplement concentrations given). In this table, growth conditions that achieve the maintenance of phmSG in an acinar-like phenotype are given.

2) Expression levels of respective genes (high, relatively high, modest, low; in comparison to expression levels in other growth media) were adopted from Jang *et al.*³⁶⁷

3) Cells grown in KGM-H (0.8 nM Ca²⁺) showed fastest and highest rates of TEER development; after 7 days, TEER showed no significant difference between cells grown in KGM-low and KGM-high.

4) In MEM medium, TEER values were below 200 Ωcm^2 .

5) Preparation of tissue biopsies and cell isolation as previously described by Tran *et al.* (2005), with some modifications.

6) The isolation and culture method for PTHSGs described by Slavik *et al.*³⁷¹ and Hegyesi *et al.*³⁶⁹ is based on the protocol of Tran *et al.*³⁶⁸ with some modifications.

abbreviations: α AMY, alpha amylase; AQP, aquaporin; BPEs, bovine pituitary extracts; β -cat, β -catenin; CK; cytokeratin (panel); Cldn, claudin; d, day; DMEM, Dulbecco's Modified Eagle Medium; E-cad, E-cadherin; EGF, epidermal growth factor; FCS, fetal calf serum; FH, fibrin hydrogel; GFR, growth factor reduced; hTERT, human telomerase reverse transcriptase; JAM-A, junctional adhesion molecule A; KGM, keratinocyte growth medium; MG, Matrigel; MUC, mucin; n.a., not analyzed; Occ, occludin; PC, polycarbonate; PET, polyester; P_{app}, apparent permeability coefficient; rER, rough endoplasmic reticulum; VIM, vimentin; ZO, zonula occludens;

the sub lingual glands 7–8%. Stimulated by usual food the salivary secretion rises to an estimated 60 mL/h; in this case the parotid glands secrete 50%, the submandibular glands 35% and the sub lingual glands 7–8%. Saliva consists of 994 g/L of water and 6 g/L dry substances, 80% of which are dissolved and 20% are suspended. The density amounts to 1.01 – 1.02 g/mL and a pH of 5.5 – 6.5 unstimulated and 7.7 stimulated.³³³

Saliva contains approximately 200 mg protein per 100 mL, including α -amylase 25–120 mg/100mL, IgA 20mg/100mL, IgG 1.5 mg/100mL and IgM 0.2mg/100mL. Antibacterial proteins in the saliva are lysozyme, lactoferrin, and sialoperoxidase and glycoproteins, muco glycoprotein 1, 2 and proline-rich glycoproteins. There are also polypeptides such as statherin and sialin and even free amino acids in saliva. The latter is in such a low concentration that extensive bacterial growth is not supported; the same goes for the glucose concentration but glucose concentration rises during food intake. The urea in saliva can be hydrolysed by bacteria leading to a higher pH. Inorganic contents are: potassium, sodium, chloride, phosphorus, bicarbonate, calcium, thiocyanate and fluoride. The composition can be different in different salivary glands and vary with the salivary flow rate.³³⁴

Barrier Studies of Salivary Gland Cell Models

Significant less *in vitro* models for salivary gland epithelia have been developed in comparison to the models for oral mucosa epithelia. A summary of salivary gland cell models as well as their applications in bioengineering is provided by Nelson *et al.*³³⁵ In Table 4 (tumor-or immortalized cells) and Table 5 (primary salivary gland epithelial cells) barrier studies with according cellular models of the salivary glands are presented in detail. Following paragraphs summarize different barrier parameters of the salivary gland epithelium *in vitro* models and their changes after specific treatments.

Tight junctions (TJs)

Regarding epithelial barrier studies of salivary glands, TJs represent the most extensively studied structure. TJs build the primary barrier against paracellular fluid and ion movement and are thus

responsible for the maintenance of cell polarity and selective transepithelial ion gradients required for saliva secretion.³³⁶ Several authors reported previously about TJ organization and expression in salivary epithelium cell models and salivary gland tissue.^{336, 337, 338, 339} A major topic of several studies is the relationship between the expression of different claudins and the corresponding barrier functionality, especially in immortalized rat salivary gland epithelial cell lines such as SMIE, SMG-C6, Par-C10 or Par-C5 (Table 4). In more detail, SMIE cells were reported to have a limited claudin expression profile, which was in line with their low barrier function, indicated by low TEER and high dextran flux. However, overexpression of claudin-4 in SMIE cells approximately doubled TEER values and decreased 70 kDa dextran flux.³⁴⁰ A barrier – regulating role of claudin-4 was also described for other salivary gland epithelial cell lines. Xiang *et al.* reported that knockdown of claudin-4 in SMG-C6 cells reversed an AMPK-induced decrease of TEER values and increase of 4 kDa FITC-dextran flux.³⁴¹ Similarly, claudin-4 is essential for modulation of paracellular permeability by muscarinic acetylcholine receptors in SMG-C6 cells.³⁴²

TEER

TEER values strongly vary between different salivary gland epithelial cell models. Highest TEER have been reported for immortalized salivary gland cell lines such as human HSDEC⁷ or rat Par-C10⁹ and Par-C5,^{343,344} the latter also referred to as Pa-4. SMG-C6, a rat submandibular gland acinar cell line, was described by several authors to develop TEER values ranging from $\sim 464 \Omega\text{cm}^2$ ⁸ to a maximum of $\sim 956 \Omega\text{cm}^2$ ³⁴⁵ when seeded on collagen – coated inserts (see Table 4). In contrast, the human neoplastic cell line HSG exhibits no or low resistances (e.g. $\sim 50 \Omega\text{cm}^2$ ³⁴⁶ $\sim 1\text{--}3 \Omega\text{cm}^2$ ³⁴⁷), but can be increased to 332–417 Ωcm^2 by appropriate insert coating such as Matrigel.³⁴⁷ However, results from studies using HSG cells should be critically questioned as it has been identified as a HeLa cross – contaminated cell line.³⁴⁸ Another tumor – derived cell line that has been studied for TEER development is CSG 120/7, originating from murine submandibular gland carcinoma, showing

an increase from day 2 with $\sim 250 \Omega\text{cm}^2$ to day 14 with an average of $2350 \Omega\text{cm}^2$.

Active Transport – Membrane transporters

Physiological expression of ATP-binding cassette (ABC) transporters in human salivary duct tissue has been described previously.³⁴⁹ Nishimura *et al.* analyzed mRNA expression profiles of 46 human ABC transporters and 108 human solute carrier (SLC) transporters in several tissues, including salivary gland.¹⁹ These studies reported expression at the protein level of major ABC transporters such as ABCB1 (P-glycoprotein) or ABCC1 and ABCC2 (MRP1, MRP2) in salivary gland ductus epithelial cells of healthy tissue, and a huge number of mRNA transcripts of almost all investigated ABC and SLC transporters. Although these data suggest a physiological role of these transporters, functionality studies of these transporters are missing in salivary glands.

Endocytic Processes

As mentioned before, either receptor – or adsorption mediated endocytosis contributes to the uptake and transport of substances across biological barriers. Several publications reported endocytic activity of salivary gland epithelial cells functioning as reuptake mechanism from primary saliva or as uptake/transcytosis from blood into saliva. For example, ferritin or BSA injected in the main excretory duct of the rat submandibular gland was taken up by light (types I and II) and dark cells or the intercalated or striated duct,^{350,351} clathrin-mediated uptake of muscarin-3 receptor and clathrin independent uptake of flotilins was proven in HSG cells,³⁵² the endocytosis of E-cadherin in salivary epithelial cells controlled by Pak1 in *Drosophila* was essential for the formation of multi-tubes in the development of salivary glands,³⁵³ the uptake of autoantibodies against Ro and La –relevant in the pathology of the Sjören's syndrome – via Fc-gamma receptors in human salivary gland cell line A-253 induced apoptosis³⁵⁴ and the presence of LRP such as LRP1B in salivary glands suggested also LRP endocytic/transcytotic activity

at the salivary gland epithelium.³⁵⁵ However, although expression and functional data *in vitro* as well as *in vivo* revealed evidence for endocytic processes at the salivary gland epithelia, only a limited number of studies and no comprehensive characterization exist.

Conclusions

The aim of this review was to provide an overview of BSB *in vitro* models and their barrier properties. In summary, many models of the oral mucosa and a smaller number of salivary gland epithelia models exist. They have been used for several different applications, cultivated under diverse conditions, but were hardly comprehensively characterized for their barrier properties. No ultimate *in vitro* model exists for any part of the BSB. Since the knowledge of the barrier properties and the corresponding cultivation conditions is the essential basis for each *in vitro* study with a model of a biological barrier, we hope that this review will help researchers to gain a valuable overview and to choose the most suitable model for their purpose. The comprehensive selection of information and data within this review also provides a starting point for future studies and the development of improved and thoroughly characterized models. In addition to the needed qualification and correlation to *in vivo* data of the *in vitro* models for the paracellular, the transport and the metabolic barrier at the expression, localization and most importantly the functionality level, future model development and validation will include the microenvironment and its influence on barrier properties. For example, Burghartz *et al.* showed recently in a 3D model the beneficial effects of the co-cultivation of salivary gland epithelial cells with microvascular endothelial cells on the barrier properties.³⁵⁶ Especially, for future 3D models such as organ-on-chips or spheroids based on e.g. hiPSC-differentiated epithelial cells co-cultivated with surrounding cells (endothelial cells, fibroblasts, etc.) a comprehensive characterization of the barrier properties will be indispensable in order to understand how close the models will be to the human *in vivo* situation.

Disclosure statement

No potential conflict of interest was reported by the authors.

ORCID

Uwe Yacine Schwarze  <http://orcid.org/0000-0002-8954-0024>

Reinhard Gruber  <http://orcid.org/0000-0001-5400-9009>

Winfried Neuhaus  <http://orcid.org/0000-0002-6552-7183>

References

- Ganz T. Epithelia: not just physical barriers. *Proc Natl Acad Sci U S A*. 2002;99(6):3357–8. doi:10.1073/pnas.072073199.
- Richter JF, et al. A novel method for imaging sites of paracellular passage of macromolecules in epithelial sheets. *J Control Release*. 2016;229:70–9. doi:10.1016/j.jconrel.2016.03.018.
- Presland RB, Jurevic RJ. Making sense of the epithelial barrier: what molecular biology and genetics tell us about the functions of oral mucosal and epidermal tissues. *J Dent Educ*. 2002;66(4):564–74.
- Li Q, et al. Interferon-gamma and tumor necrosis factor-alpha disrupt epithelial barrier function by altering lipid composition in membrane microdomains of tight junction. *Clin Immunol*. 2008;126(1):67–80. doi:10.1016/j.clim.2007.08.017.
- Ye D, Ma I, Ma TY. Molecular mechanism of tumor necrosis factor-alpha modulation of intestinal epithelial tight junction barrier. *Am J Physiol Gastrointest Liver Physiol*. 2006;290(3):G496–504. doi:10.1152/ajpgi.00318.2005.
- Ma TY, et al. TNF-alpha-induced increase in intestinal epithelial tight junction permeability requires NF-kappa B activation. *Am J Physiol Gastrointest Liver Physiol*. 2004;286(3):G367–76. doi:10.1152/ajpgi.00173.2003.
- Abe A, et al. Interferon-gamma increased epithelial barrier function via upregulating claudin-7 expression in human submandibular gland duct epithelium. *J Mol Histol*. 2016;47(3):353–63. doi:10.1007/s10735-016-9667-2.
- Mei M, et al. Claudin-3 is required for modulation of paracellular permeability by TNF- α through ERK1/2/slug signaling axis in submandibular gland. *Cell Signal*. 2015;27:10. doi:10.1016/j.cellsig.2015.07.002.
- Baker OJ, et al. Proinflammatory cytokines tumor necrosis factor-alpha and interferon-gamma alter tight junction structure and function in the rat parotid gland Par-C10 cell line. *Am J Physiol Cell Physiol*. 2008;295(5):C1191–201. doi:10.1152/ajpcell.00144.2008.
- Banks WA. From blood-brain barrier to blood-brain interface: new opportunities for CNS drug delivery. *Nat Rev Drug Discov*. 2016;15(4):275–92. doi:10.1038/nrd.2015.21.
- Wigley C. Chapter 33, Oral Cavity. [book auth.] *Standing S Berkovitz BKB. Gray's Anatomy*. 2005:581–606. 39.
- Salamat-Miller N, Chittchang M, Johnston TP. The use of mucoadhesive polymers in buccal drug delivery. *Adv Drug Deliv Rev*. 2005;57(11):1666–91. doi:10.1016/j.addr.2005.07.003.
- Reddy PC, Chaitanya KSC, Madhusudan Rao Y. A review on bioadhesive buccal drug delivery systems: current status of formulation and evaluation methods. *Daru*. 2011;19(6):385–403.
- Kulkarni UD, et al. Effect of Experimental Temperature on the Permeation of Model Diffusants Across Porcine Buccal Mucosa. *AAPS PharmSciTech*. 2011;12(2):579–86. doi:10.1208/s12249-011-9624-z.
- Consortium, International Transporter, et al. Membrane transporters in drug development. *Nat Rev Drug Discov*. 2010;9(3):215–36. doi:10.1038/nrd3028.
- Li Y, Lu J, Paxton JW. The role of ABC and SLC transporters in the pharmacokinetics of dietary and herbal phytochemicals and their interactions with xenobiotics. *Curr Drug Metab*. 2012;13(5):624–39. doi:10.2174/1389200211209050624.
- Lin L, et al. SLC transporters as therapeutic targets: emerging opportunities. *Nat Rev Drug Discov*. 2015;14(8):543–60. doi:10.1038/nrd4626.
- Morrissey KM, et al. The UCSF-FDA TransPortal: a public drug transporter database. *Clin Pharmacol Ther*. 2012;92(5):545–6. doi:10.1038/clpt.2012.44.
- Nishimura M, Naito S. Tissue-specific mRNA expression profiles of human ATP-binding cassette and solute carrier transporter superfamilies. *Drug Metab Pharmacokinet*. 2005;20(6):452–77. doi:10.2133/dmpk.20.452.
- DeGorter MK, et al. Drug transporters in drug efficacy and toxicity. *Annu Rev Pharmacol Toxicol*. 2012(52):249–73. doi:10.1146/annurev-pharmtox-010611-134529.
- Nigam SK. What do drug transporters really do? *Nat Rev Drug Discov*. 2015;14(1):29–44. doi:10.1038/nrd4461.
- Nałęcz KA. Solute Carriers in the Blood-Brain Barrier: Safety in Abundance. *Neurochem Res*. 2016; 42(3):795–809. doi:10.1007/s11064-016-2030-x.
- Mahringer A, Fricker G. ABC transporters at the blood-brain barrier. *Expert Opin Drug Metab Toxicol*. 12(5):499–508. doi:10.1517/17425255.2016.1168804.
- Seeger MA, van Veen HW. Molecular basis of multidrug transport by ABC transporters. *Biochim Biophys Acta*. 2009;1794(5):725–37. doi:10.1016/j.bbapap.2008.12.004.
- Tarling EJ, de Aguiar Vallim TQ, Edwards PA. Role of ABC transporters in lipid transport and human disease. *Trends Endocrinol Metab*. 2013;24(7):342–50. doi:10.1016/j.tem.2013.01.006.
- Kaminski WE, Piehler A, Wenzel JJ. ABC A-subfamily transporters: structure, function and disease. *Biochim Biophys Acta*. 2006;1762(5):510–24. doi:10.1016/j.bbadis.2006.01.011.
- Hediger MA, et al. The ABCs of membrane transporters in health and disease (SLC series): introduction.

- Mol Aspects Med. 2013; 34 (2–3): 95–107. doi:10.1016/j.mam.2012.12.009.
28. Kulkarni PS, et al. Characterization of human buccal epithelial cells transfected with the simian virus 40 T-antigen gene. *Carcinogenesis*. 1995;16(10):2515–21. doi:10.1093/carcin/16.10.2515.
 29. Tsukita S, Furuse M, Itoh M. Multifunctional strands in tight junctions. *Nat Rev Mol Cell Biol*. 2001;2(4):285–93. doi:10.1038/35067088.
 30. Zihni C, et al. Tight junctions: from simple barriers to multifunctional molecular gates. *Nat Rev Mol Cell Biol*. 2016;17(9):564–80. doi:10.1038/nrm.2016.80.
 31. Mineta K, Yamamoto Y, Yamazaki Y, Tanaka H, Tada Y, Saito K, Tamura A, Igarashi M, Endo T, Takeuchi K, Tsukita S. Predicted expansion of the claudin multi-gene family. *FEBS Lett*. 2011;18;585(4):606–12. doi:10.1016/j.febslet.2011.01.028.
 32. Günzel D, Fromm M. Claudins and other tight junction proteins. *Compr Physiol*. 2012;2(3):1819–52. 2012.
 33. Canfield SG, Stebbins MJ, Morales BS, Asai SW, Vatine GD, Svendsen CN, Palecek SP, Shusta EV. An isogenic blood-brain barrier model comprising brain endothelial cells, astrocytes, and neurons derived from human induced pluripotent stem cells. *J Neurochem*. 2017;140(6):874–88. doi:10.1111/jnc.13923.
 34. Appelt-Menzel A, Cubukova A, Günther K, Edenhofer F, Piontek J, Krause G, Stüber T, Walles H, Neuhaus W, Metzger M. Establishment of a Human Blood-Brain Barrier Co-culture Model Mimicking the Neurovascular Unit Using Induced Pluri- and Multipotent Stem Cells. *Stem Cell Reports*. 2017;8(4):894–906. doi:10.1016/j.stemcr.2017.02.021.
 35. Matoltsy AG, Parakkal PF. Membrane-coating granules of keratinizing epithelia. *J Cell Biol*. 1965;24:297–307. doi:10.1083/jcb.24.2.297.
 36. Hayward AF. Membrane-coating granules. *Int Rev Cytol*. 1979;95:97–127. doi:10.1016/S0074-7696(08)61661-7.
 37. Alberts B, Johnson A, Lewis J, et al. *Molecular Biology of the Cell*. 4th edition. s.l.: New York: Garland Science; 2002.
 38. Yasen A, Herrera R, Rosbe K, Lien K, Tugizov SM. HIV internalization into oral and genital epithelial cells by endocytosis and macropinocytosis leads to viral sequestration in the vesicles. *Virology*. 2018;515:92–107. doi:10.1016/j.virol.2017.12.012.
 39. Drago L, Mombelli B, De Vecchi E, Bonaccorso C, Fassina MC, Gismodo MR. *Candida albicans* cellular internalization: a new pathogenic factor? *Int J Antimicrob Agents*. 2000;6(4):545–7. doi:10.1016/S0924-8579(00)00296-X.
 40. Solis NV, Swidergall M, Bruno VM, Gaffen SL, Filler SG. The Aryl-Hydrocarbon Receptor governs epithelial cell invasion during oropharyngeal candidiasis. *MBio*. 2017;8(2), pii: e00025–17. doi:10.1128/mBio.00025-17.
 41. Michalczyk A, Varigos G, Smith L, Ackland ML. Fresh and cultured buccal cells as a source of mRNA and protein for molecular analysis. *Biotechniques*. 2004;37(2):262–4,266–9. 37(2):262–4, 266–9, 2004. doi:10.2144/04372RR03.
 42. Takeuchi H, Furuta N, Morisaki I, Amano A. Exit of intracellular *Porphyromonas gingivalis* from gingival epithelial cells is mediated by endocytic recycling pathway. *Cell Microbiol*. 2011;13(5):677–91. doi:10.1111/j.1462-5822.2010.01564.x.
 43. Du W, Fan Y, Zheng N, He B, Yuan L, Zhang H, Wang X, Wang J, Zang X, Zhang Q. Transferrin receptor specific nanocarriers conjugated with functional 7peptide for oral delivery. *Biomaterials*. 2013;34(3):794–806. doi:10.1016/j.biomaterials.2012.10.003.
 44. Ivanov AI, Nusrat A, Parkos CA. Endocytosis of the apical junctional complex: mechanisms and possible roles in regulation of epithelial barriers. *Bioessays*. 2005;27(4):356–65. doi:10.1002/bies.20203.
 45. Utech M, et al. Mechanism of IFN-gamma-induced endocytosis of tight junction proteins: myosin II-dependent vacuolarization of the apical plasma membrane. *Mol Biol Cell*. 2005;16(10):5040–52. doi:10.1091/mbc.e05-03-0193.
 46. Harhaj NS, Barber AJ, Antonetti DA. Platelet-derived growth factor mediates tight junction redistribution and increases permeability in MDCK cells. *J Cell Physiol*. 2002;193(3):349–64. doi:10.1002/jcp.10183.
 47. Hopkins AM, et al. Constitutive activation of Rho proteins by CNF-1 influences tight junction structure and epithelial barrier function. *J Cell Sci*. 2003;116(Pt 4):725–42. doi:10.1242/jcs.00300.
 48. Kowalczyk AP, Nanes BA. Adherens junction turnover: regulating adhesion through cadherin endocytosis, degradation, and recycling. *Subcell Biochem*. 2012(60):197–222. doi:10.1007/978-94-007-4186-7_9.
 49. Linden SK, et al. Mucins in the mucosal barrier to infection. *Mucosal Immunol*. 2008;1(3):183–97. doi:10.1038/mi.2008.5.
 50. Alemka A, Corcionivoschi N, Bourke B. Defense and adaptation: the complex inter-relationship between *Campylobacter jejuni* and mucus. *Front Cell Infect Microbiol*. 2012;2:15. doi:10.3389/fcimb.2012.00015.
 51. Corfield AP. Mucins: a biologically relevant glycan barrier in mucosal protection. *Biochim Biophys Acta*. 2015;1850(1):236–52. doi:10.1016/j.bbagen.2014.05.003.
 52. Dodds M, et al. Saliva A review of its role in maintaining oral health and preventing dental disease. *BDJ Team*. 2015;2. doi:10.1038/bdjteam.2015.123.
 53. Marcotte H, Lavoie MC. Oral microbial ecology and the role of salivary immunoglobulin A. *Microbiol Mol Biol Rev*. 1998;62(1):71–109.
 54. McGuckin MA, et al. Mucin dynamics and enteric pathogens. *Nat Rev Microbiol*. 2011;9(4):265–78. doi:10.1038/nrmicro2538.
 55. Benson K, Cramer S, Galla HJ. Impedance-based cell monitoring: barrier properties and beyond. *Fluids Barriers CNS*. 2013;10(1):5. doi:10.1186/2045-8118-10-5.
 56. Tanaka H, Yamamoto Y, Kashihara H, Yamazaki Y, Tani K, Fujiyoshi Y, Mineta K, Takeuchi K, Tamura A, Tsukita S. Claudin-21 Has a Paracellular Channel Role at Tight Junctions. *Molecular and Cellular Biology*. 2016;36:954–64. doi:10.1128/MCB.00758-15.

57. Günzel D, Yu ASL. Claudins and the modulation of tight junction permeability. *Physiol Rev.* 2013;93:525–69. doi:10.1152/physrev.00019.2012.
58. Srinivasan B, et al. TEER measurement techniques for in vitro barrier model systems. *J Lab Autom.* 2015;20(2):107–26. doi:10.1177/2211068214561025.
59. Neuhaus W, Bogner E, Wirth M, Trzeciak J, Lachmann B, Gabor F, Noe CR. A novel tool to characterize paracellular transport: the APTS-dextran ladder. *Pharm Res.* 2006;23(7):1491–501. doi:10.1007/s11095-006-0256-z.
60. Sun H, Pang KS. Permeability, transport, and metabolism of solutes in Caco-2 cell monolayers: a theoretical study. *Drug Metab Dispos.* 2008;36(1):102–23. doi:10.1124/dmd.107.015321.
61. Neuhaus W. Development and validation of in-vitro models of the blood-brain barrier. *Dissertation.* Vienna: s.n., 2007.
62. Rupniak HT, et al. Characteristics of four new human cell lines derived from squamous cell carcinomas of the head and neck. *J Natl Cancer Inst.* 1985;75(4):621–35.
63. Jacobsen J, et al. TR146 cells grown on filters as a model for human buccal epithelium: I. Morphology, growth, barrier properties, and permeability. *Int J Pharm.* 1995;125:165–84. doi:10.1016/0378-5173(95)00109-V.
64. Jacobsen J, et al. Filter-grown TR146 cells as an in vitro model of human buccal epithelial permeability. *Eur J Oral Sci.* 1999;107(2):138–46. doi:10.1046/j.0909-8836.1999.eos107210.x.
65. Nielsen HM, et al. TR146 cells grown on filters as a model of human buccal epithelium: permeability of fluorescein isothiocyanate-labelled dextrans in the presence of sodium glycocholate. *J Control Release.* 1999;60;(2-3):223–33. doi:10.1016/S0168-3659(99)00081-4.
66. Nielsen HM, Rassing MR. TR146 cells grown on filters as a model of human buccal epithelium: V. Enzyme activity of the TR146 cell culture model, human buccal epithelium and porcine buccal epithelium, and permeability of leu-enkephalin. *Int J Pharm.* 2000;200(2):261–70. doi:10.1016/S0378-5173(00)00394-X.
67. Nielsen HM, Rassing MR. Nicotine permeability across the buccal TR146 cell culture model and porcine buccal mucosa in vitro: Effect of pH and concentration. *Eur J Pharm Sci.* 2002;16(3):151–7. doi:10.1016/S0928-0987(02)00083-0.
68. Nielsen HM, Rassing MR. TR146 cells grown on filters as a model of human buccal epithelium: IV. Permeability of water, mannitol, testosterone and beta-adrenoceptor antagonists. Comparison to human, monkey and porcine buccal mucosa. *Int J Pharm.* 2000;194(2):155–67. doi:10.1016/S0378-5173(99)00368-3.
69. Gumbleton M, Audus KL. Progress and limitations in the use of in vitro cell cultures to serve as a permeability screen for the blood-brain barrier. *J Pharm Sci.* 2001;90(11):1681–98. doi:10.1002/jps.1119.
70. Deli MA, et al. Permeability studies on in vitro blood-brain barrier models: physiology, pathology, and pharmacology. *Cell Mol Neurobiol.* 2005;25(1):59–127. doi:10.1007/s10571-004-1377-8.
71. Zhang H, Zhang J, Streisand JB. Oral mucosal drug delivery: clinical pharmacokinetics and therapeutic applications. *Clin Pharmacokinet.* 2002;41(9):661–80. doi:10.2165/00003088-200241090-00003.
72. Sander C, Nielsen HM, Jacobsen J. Buccal delivery of metformin: TR146 cell culture model evaluating the use of bioadhesive chitosan discs for drug permeability enhancement. *Int J Pharm.* 2013;458(2):254–61. doi:10.1016/j.ijpharm.2013.10.026.
73. Portero A, Remuñán-López C, Nielsen HM. The potential of chitosan in enhancing peptide and protein absorption across the TR146 cell culture model-an in vitro model of the buccal epithelium. *Pharm Res.* 2002;19(2):169–74. doi:10.1023/A:1014220832384.
74. Klemetsrud T, et al. Polymer coated liposomes for use in the oral cavity - A study of the in vitro toxicity, effect on cell permeability and interaction with mucin. *J Liposome Res.* 2016;3:1–37.
75. Iyire A, Alayedi M and Mohammed AR. Pre-formulation and systematic evaluation of amino acid assisted permeability of insulin across in vitro buccal cell layers. *Sci Rep.* 2016;6:32498. doi:10.1038/srep32498.
76. Pistone S, et al. Formulation of polysaccharide-based nanoparticles for local administration into the oral cavity. *Eur J Pharm Sci.* 2016;96:381–9. doi:10.1016/j.ejps.2016.10.012.
77. Kaiser M, et al. In Vitro and Sensory Evaluation of Capsaicin-Loaded Nanoformulations. *PLoS One.* 2015;10:10. doi:10.1371/journal.pone.0141017.
78. Zeng N, et al. Poloxamer bioadhesive hydrogel for buccal drug delivery: Cytotoxicity and trans-epithelial permeability evaluations using TR146 human buccal epithelial cell line. *Int J Pharm.* 2015;495(2):1028–37. doi:10.1016/j.ijpharm.2015.09.045.
79. Caon T, et al. Enhancing the buccal mucosal delivery of peptide and protein therapeutics. *Pharm Res.* 2015;32(1):1–21. doi:10.1007/s11095-014-1485-1.
80. Park K, Morishita M. Biodrug Delivery Systems: fundamentals, applications and clinical development. [Online] [Cited: November 28, 2016]. <https://books.google.at/books?id=91jvBQAAQBAJ&pg=PA122&lpg=PA122&dq=buccal+mucosa+barrier&source=bl&ots=pLjmJZyF2e&sig=gtj0OLOHtmyjGTzSADGWn6Q0LIw&hl=de&sa=X&ved=0ahUKEwj4pdTu78DQAhUFLsAKHfvIAAIQ6AEIVTAL#v=onepage&q=buccal%20mucosa%20barrier&f=false>.
81. Sohi H, et al. Critical evaluation of permeation enhancers for oral mucosal drug delivery. *Drug Dev Ind Pharm.* 2010;36(3):254–82. doi:10.3109/03639040903117348.
82. Lermann U, Morschhäuser J. Secreted aspartic proteases are not required for invasion of reconstituted human epithelia by *Candida albicans*. *Microbiology.*

- 2008;154(Pt 11):3281–3295. doi:10.1099/mic.0.2008/022525-0.
83. Moyes DL, et al. A biphasic innate immune MAPK response discriminates between the yeast and hyphal forms of *Candida albicans* in epithelial cells. *Cell Host Microbe*. 2010;8(3):225–35. doi:10.1016/j.chom.2010.08.002.
84. Samaranyake YH, et al. Differential phospholipase gene expression by *Candida albicans* in artificial media and cultured human oral epithelium. *APMIS*. 2006;114(12):857–66. doi:10.1111/j.1600-0463.2006.apm_479.x.
85. Senel S, et al. Enhancing effect of chitosan on peptide drug delivery across buccal mucosa. 2000;21(20):2067–71.
86. Wertz PW, Squier CA. Cellular and molecular basis of barrier function in oral epithelium. *Crit Rev Ther Drug Carrier Syst*. 1991;8(3):237–69.
87. Teubl BJ, et al. The oral cavity as a biological barrier system: design of an advanced buccal in vitro permeability model. *Eur J Pharm Biopharm*. 2013;84(2):386–93. doi:10.1016/j.ejpb.2012.10.021.
88. Cone RA. Barrier properties of mucus. *Adv Drug Deliv Rev*. 2009;61(2):75–85. doi:10.1016/j.addr.2008.09.008.
89. Yadav NP, et al. Evaluation of tissue engineered models of the oral mucosa to investigate oral candidiasis. *Microb Pathog*. 2011;50(6):278–85. doi:10.1016/j.micpath.2010.11.009.
90. Miyauchi S, et al. Establishment of human tumor cell line (Ueda-1) derived from squamous cell carcinoma of the floor of the mouth. *Jpn J Oral Maxillofac Surg*. 1985;31:1347–51. in Japanese, not available. doi:10.5794/jjoms.31.1347.
91. Wang Y, et al. Evaluation of HO-1-u-1 cell line as an in vitro model for sublingual drug delivery involving passive diffusion—Initial validation studies. *Int J Pharm*. 2007; 334(1–2): 27–34. doi:10.1016/j.ijpharm.2006.10.012.
92. Narang N, Sharma J. Sublingual Mucosa as a route for systemic drug delivery. *Int J Pharm Pharmaceutical Sci*. 2011;3(2):18–22.
93. Wang Y, Zuo Z, Chow MS. HO-1-u-1 model for screening sublingual drug delivery—Influence of pH, osmolarity and permeation enhancer. *Int J Pharm*. 2009; 370(1–2): 68–74. doi:10.1016/j.ijpharm.2008.11.010.
94. Hiroshima Y, et al. Effect of Hangeshashinto on calprotectin expression in human oral epithelial cells. *Odontology*. 2016;104(2):152–62. doi:10.1007/s10266-015-0196-3.
95. O’Callaghan K, et al. Induction of apoptosis in oral squamous carcinoma cells by pyrrolo-1,5-benzoxazepines. *Mol Med Rep*. 2015;12(3):3748–54. doi:10.3892/mmr.2015.3832.
96. Khammanivong A, et al. S100A8/A9 (calprotectin) negatively regulates G2/M cell cycle progression and growth of squamous cell carcinoma. *PLoS One*. 2013;8:7. doi:10.1371/journal.pone.0069395.
97. Lermann U, Morschhäuser J. Secreted aspartic proteases are not required for invasion of reconstituted human epithelia by *Candida albicans*. *Microbiology*. 2008;154(Pt 11):3281–95. doi:10.1099/mic.0.2008/022525-0.
98. Reiss M, Pitman SW, Sartorelli AC. Modulation of the terminal differentiation of human squamous carcinoma cells in vitro by all-trans-retinoic acid. *J Natl Cancer Inst*. 1985;74(5):1015–23.
99. Hansson A, et al. Expression of keratins in normal, immortalized and malignant oral epithelia in organotypic culture. *Oral Oncol*. 2001;37(5):419–30. doi:10.1016/S1368-8375(00)00089-0.
100. Ceder R, et al. The application of normal, SV40 T-antigen-immortalised and tumour-derived oral keratinocytes, under serum-free conditions, to the study of the probability of cancer progression as a result of environmental exposure to chemicals. *Altern Lab Anim*. 2007;35(6):621–39.
101. Whang YM, et al. Hyperacetylation enhances the growth-inhibitory effect of all-trans retinoic acid by the restoration of retinoic acid receptor beta expression in head and neck squamous carcinoma (HNSCC) cells. *Cancer Chemother Pharmacol*. 2005;56(5):543–55. doi:10.1007/s00280-004-0970-3.
102. Sarang Z, et al. Microarray assessment of fibronectin, collagen and integrin expression and the role of fibronectin-collagen coating in the growth of normal, SV40 T-antigen-immortalised and malignant human oral keratinocytes. *Altern Lab Anim*. 2003;31(6):575–85.
103. Chun SG, et al. Targeted inhibition of histone deacetylases and hedgehog signaling suppress tumor growth and homologous recombination in aerodigestive cancers. *Am J Cancer Res*. 2015;5(4):1337–52.
104. Moroyama T, et al. Establishment and characterization of a human tumor cell line (Nakata-1) derived from squamous carcinoma of the buccal mucosa. *Proc Jpn Can Assoc*. 1986;45:242. not available.
105. Sato K, et al. RANKL synthesized by both stromal cells and cancer cells plays a crucial role in osteoclastic bone resorption induced by oral cancer. *Am J Pathol*. 2013;182(5):1890–9. doi:10.1016/j.ajpath.2013.01.038.
106. Ohshima M, et al. Physiologic levels of epidermal growth factor in saliva stimulate cell migration of an oral epithelial cell line, HO-1-N-1. *Eur J Oral Sci*. 2002;110(2):130–6. doi:10.1034/j.1600-0722.2002.11179.x.
107. Laheij AM, et al. The impact of virulence factors of *Porphyromonas gingivalis* on wound healing in vitro. *J Oral Microbiol*. 2015;7:27543. doi:10.3402/jom.v7.27543.
108. Hayashi K, et al. Effect of 9-cis-retinoic acid on oral squamous cell carcinoma cell lines. *Cancer Lett*. 2000;151(2):199–208. doi:10.1016/S0304-3835(99)00422-X.
109. Hayashi K, et al. Overexpression of retinoic acid receptor beta induces growth arrest and apoptosis in oral cancer cell lines. *Jpn J Cancer Res*. 2001;92(1):42–50. doi:10.1111/j.1349-7006.2001.tb01046.x.

110. Prime SS, et al. The behaviour of human oral squamous cell carcinoma in cell culture. *J Pathol.* 1990;160(3):259–69. doi:10.1002/path.1711600313.
111. Yee M, et al. Porphyromonas gingivalis stimulates IL-6 and IL-8 secretion in GSM-K, HSC-3 and H413 oral epithelial cells. *Anaerob.* 2014;28:62–7. doi:10.1016/j.anaerobe.2014.05.011.
112. Guo W, et al. CD24 activates the NLRP3 inflammasome through c-Src kinase activity in a model of the lining epithelium of inflamed periodontal tissues. *Immun Inflamm Dis.* 2014;2(4):239–53. doi:10.1002/iid3.40.
113. Ye P. Modulation of epithelial tight junctions by TGF-beta 3 in cultured oral epithelial cells. *Aust Dent J.* 2012;57(1):11–7. doi:10.1111/j.1834-7819.2011.01651.x.
114. Narayanan SP, et al. Integrated genomic analyses identify KDM1A's role in cell proliferation via modulating E2F signaling activity and associate with poor clinical outcome in oral cancer. *Cancer Lett.* 2015;367(2):162–72. doi:10.1016/j.canlet.2015.07.022.
115. Ye P, et al. Differential expression of transforming growth factors-beta 1, -beta 2, -beta 3 and the type I, II, III receptors in the lining epithelia of inflamed gingiva. *Pathology.* 2003;35(5):384–92. doi:10.1080/00313020310001602585.
116. Lee EJ, et al. Characterization of newly established oral cancer cell lines derived from six squamous cell carcinoma and two mucoepidermoid carcinoma cells. *Exp Mol Med.* 2005;37(5):379–90. doi:10.1038/emm.2005.48.
117. Kim YK, Koo NY, Yun PY. Anticancer effects of CKD-602 (Camtobell®) via G2/M phase arrest in oral squamous cell carcinoma cell lines. *Oncol Lett.* 2015;9(1):136–42. doi:10.3892/ol.2014.2648.
118. Cho JH, et al. The bacterial protein azurin enhances sensitivity of oral squamous carcinoma cells to anticancer drugs. *Yonsei Med J.* 2011;52(5):773–8. doi:10.3349/ymj.2011.52.5.773.
119. Park SR, et al. Pseudomonas aeruginosa exotoxin A reduces chemoresistance of oral squamous carcinoma cell via inhibition of heat shock proteins 70 (HSP70). *Yonsei Med J.* 2010;51:5. doi:10.3349/ymj.2010.51.5.708.
120. Moon, Y, et al. Effect of CD133 overexpression on the epithelial-to-mesenchymal transition in oral cancer cell lines. *Clin Exp Metastasis.* 2016;33(5):487–96. doi:10.1007/s10585-016-9793-y.
121. Lin, SC, et al. Establishment of OC3 oral carcinoma cell line and identification of NF-kappa B activation responses to areca nut extract. *J Oral Pathol Med.* 2004;33(2):79–86. doi:10.1111/j.1600-0714.2004.00034.x.
122. Chen, YH, et al. Apoptotic effect of cisplatin and cordycepin on OC3 human oral cancer cells. *Chin J Integr Med.* 2014;20(8):624–32. doi:10.1007/s11655-013-1453-3.
123. Wu, SY, Wu, AT, Liu, SH. MicroRNA-17-5p regulated apoptosis-related protein expression and radiosensitivity in oral squamous cell carcinoma caused by betel nut chewing. *Oncotarget.* 2016;7(32):51482–51493. doi:10.18632/oncotarget.9856.
124. Hsiao, JR, Leu, SF, Huang, BM. Apoptotic mechanism of paclitaxel-induced cell death in human head and neck tumor cell lines. *J Oral Pathol Med.* 2009;38(2):188–97. doi:10.1111/j.1600-0714.2008.00732.x.
125. Wang, SH, Chang, CW, Chou, HC. 5-Methoxytryptophan-dependent inhibition of oral squamous cell carcinoma metastasis. *Electrophoresis.* 2015;36(17), pp. 2027–34. doi:10.1002/elps.201500154.
126. Kok, SH, et al. Establishment and characterization of a tumorigenic cell line from areca quid and tobacco smoke-associated buccal carcinoma. *Oral Oncol.* 2007;43(7):639–47. doi:10.1016/j.oraloncology.2006.07.007.
127. Lin, CS, et al. Silencing JARID1B suppresses oncogenicity, stemness and increases radiation sensitivity in human oral carcinoma. 2015;368(1):36–45.
128. Lee, CH, et al. IL-1β promotes malignant transformation and tumor aggressiveness in oral cancer. *J Cell Physiol.* 2015;230(4):875–84. doi:10.1002/jcp.24816.
129. Chang, CC, et al. MicroRNA-17/20a functions to inhibit cell migration and can be used a prognostic marker in oral squamous cell carcinoma. *Oral Oncol.* 2013;49(9):923–31. doi:10.1016/j.oraloncology.2013.03.430.
130. Chang, CC, et al. HDAC2 promotes cell migration/invasion abilities through HIF-1α stabilization in human oral squamous cell carcinoma. *J Oral Pathol Med.* 2011;40(7):567–75. doi:10.1111/j.1600-0714.2011.01009.x.
131. Gioanni, J, et al. Two new human tumor cell lines derived from squamous cell carcinomas of the tongue: establishment, characterization and response to cytotoxic treatment. *Eur J Cancer Clin Oncol.* 1988;24(9):1445–55. doi:10.1016/0277-5379(88)90335-5.
132. Zhang, Z, et al. Hyaluronan synthase 2 expressed by cancer-associated fibroblasts promotes oral cancer invasion. 2016;35(1):181. doi:10.1186/s13046-016-0458-0.
133. Li, YC, et al. SATB1 promotes tumor metastasis and invasiveness in oral squamous cell carcinoma. *Oral Dis.* 2016; 23(2):247–254. doi:10.1111/odi.12602.
134. Zhang, X, et al. Knockdown of Myosin 6 inhibits proliferation of oral squamous cell carcinoma cells. *J Oral Pathol Med.* 2016;45(10):740–5. doi:10.1111/jop.12448.
135. Bozec, A, et al. Combination of phosphatidylinositol-3-kinase targeting with cetuximab and irradiation: A preclinical study on an orthotopic xenograft model of head and neck cancer. *Head Neck.* 2017;39(1):151–159. doi:10.1002/hed.24560.
136. Tonissi, F, et al. Reoxygenation Reverses Hypoxia-related Radioresistance in Head and Neck Cancer Cell Lines. 2016;36(5):2211–5.
137. Stojanović, N, et al. Integrin αvβ3 expression in tongue squamous carcinoma cells Cal27 confers anticancer drug resistance through loss of pSrc(Y418). *Biochim Biophys Acta.* 2016;1863(8):1969–78. doi:10.1016/j.bbamcr.2016.04.019.

138. Mo, H, et al. Expression, roles and therapy target values of CD24 in oral squamous cell carcinoma. *Beijing Da Xue Xue Bao*. 2016;48(1):16–22. Article in Chinese.
139. Ma, Z, Bi, Q and Wang, Y. Hydrogen sulfide accelerates cell cycle progression in oral squamous cell carcinoma cell lines. *Oral Dis*. 2015;21(2):156–62. doi:10.1111/odi.12223.
140. Cui, Z, et al. TRIM24 overexpression is common in locally advanced head and neck squamous cell carcinoma and correlates with aggressive malignant phenotypes. *PLoS One*. 2013;8(5):e63887. doi:10.1371/journal.pone.0063887.
141. Wu, HH, et al. Bevacizumab regulates cancer cell migration by activation of STAT3. *Asian Pac J Cancer Prev*. 2015;16(5):6501–6. doi:10.7314/APJCP.2015.16.15.6501.
142. Cheung, J, et al. A nonviral vector with transfection activity comparable with adenoviral transduction. *Ther Deliv*. 2016;7(11):739–49. doi:10.4155/tde-2016-0054.
143. Sapkota, D, et al. S100A16 promotes differentiation and contributes to a less aggressive tumor phenotype in oral squamous cell carcinoma. *BMC Cancer*. 2015;15:631. doi:10.1186/s12885-015-1622-1.
144. Samal, SK, et al. Ketorolac salt is a newly discovered DDX3 inhibitor to treat oral cancer. *Sci Rep*. 2015;5:9982. doi:10.1038/srep09982.
145. Rheinwald, JG and Beckett, MA. Tumorigenic keratinocyte lines requiring anchorage and fibroblast support cultured from human squamous cell carcinomas. *Cancer Res*. 1981;41(5):1657–63.
146. Otsuka, Y, et al. High expression of EPB41L5, an integral component of the Arf6-driven mesenchymal program, correlates with poor prognosis of squamous cell carcinoma of the tongue. *Cell Commun Signal*. 2016;14(1):28. doi:10.1186/s12964-016-0151-0.
147. Kadletz, L, et al. AZD5582, an IAP antagonist that leads to apoptosis in head and neck squamous cell carcinoma cell lines and is eligible for combination with irradiation. *Acta Otolaryngol*. 2016; 137(3):320–325. doi:10.1080/00016489.2016.1242776.
148. McGregor, F, et al. Molecular changes associated with oral dysplasia progression and acquisition of immortality: potential for its reversal by 5-azacytidine. *Cancer Res*. 2002;62(16):4757–66.
149. Colley, HE, et al. Development of tissue-engineered models of oral dysplasia and early invasive oral squamous cell carcinoma. *Br J Cancer*. 2011;105(10):1582–92. doi:10.1038/bjc.2011.403.
150. Gaballah, K, et al. Tissue engineering of oral dysplasia. *J Pathol*. 2008;215(3):280–9. doi:10.1002/path.2360.
151. Gaballah, K, et al. Lysis of Dysplastic but not Normal Oral Keratinocytes and Tissue-Engineered Epithelia with Conditionally Replicating Adenoviruses. *Cancer Res*. 2007;67(15):7284–94. doi:10.1158/0008-5472.CAN-06-3834.
152. Mian, SA, et al. Raman spectroscopy can discriminate between normal, dysplastic and cancerous oral mucosa: a tissue-engineering approach. *J Tissue Eng Regen Med*. 2016; 11(11):3253–3262. doi:10.1002/term.2234.
153. Chang, SE, et al. DOK, a cell line established from human dysplastic oral mucosa, shows a partially transformed non-malignant phenotype. *Int J Cancer*. 1992;52(6):896–902. doi:10.1002/ijc.2910520612.
154. Kulasekara, KK, et al. Cancer progression is associated with increased expression of basement membrane proteins in three-dimensional in vitro models of human oral cancer. *Arch Oral Biol*. 2009;54(10):924–31. doi:10.1016/j.archoralbio.2009.07.004.
155. Rajendiran, S, et al. MIEN1 promotes oral cancer progression and implicates poor overall survival. *Cancer Biol Ther*. 2015;16(6):876–85. doi:10.1080/15384047.2015.1040962.
156. Dalley, AJ, et al. Organotypic culture of normal, dysplastic and squamous cell carcinoma-derived oral cell lines reveals loss of spatial regulation of CD44 and p75 NTR in malignancy. *J Oral Pathol Med*. 2013;42(1):37–46. doi:10.1111/j.1600-0714.2012.01170.x.
157. Chan LP, et al. IL-8 promotes HNSCC progression on CXCR1/2-mediated NOD1/RIP2 signaling pathway. *Oncotarget*. 2016; 7(38):61820–61831. doi:10.18632/oncotarget.11445.
158. Dong Y, et al. Establishment of a new OSCC cell line derived from OLK and identification of malignant transformation-related proteins by differential proteomics approach. *Sci Rep*. 2015;5:12668. doi:10.1038/srep12668.
159. Rikimaru, K, et al. Growth of the malignant and non-malignant human squamous cells in a protein-free defined medium. *In Vitro Cell Dev Biol*. 1990;26(9):849–56. doi:10.1007/BF02624609.
160. Harada, K, et al. Metformin in combination with 5-fluorouracil suppresses tumor growth by inhibiting the Warburg effect in human oral squamous cell carcinoma. *Int J Oncol*. 2016;49(1):276–84. doi:10.3892/ijo.2016.3523.
161. Pal, SK, et al. THBS1 is induced by TGFβ1 in the cancer stroma and promotes invasion of oral squamous cell carcinoma. *J Oral Pathol Med*. 2016;45(10):730–9. doi:10.1111/jop.12430.
162. Ketkaew, Y, et al. Apigenin inhibited hypoxia induced stem cell marker expression in a head and neck squamous cell carcinoma cell line. *Arch Oral Biol*. 74:69–74. doi:10.1016/j.archoralbio.2016.11.010.
163. Momose, F, et al. Variant sublines with different metastatic potentials selected in nude mice from human oral squamous cell carcinomas. *J Oral Pathol Med*. 1989; 18(7):391–5. doi:10.1111/j.1600-0714.1989.tb01570.x.

164. Yuan, Z, et al. Overexpression of HOXB7 protein reduces sensitivity of oral cancer cells to chemo-radiotherapy. *Cancer Gene Ther.* 2016;23:12:419–24. doi:10.1038/cgt.2016.55.
165. Kaneko, T, et al. Hypoxia-induced epithelial-mesenchymal transition is regulated by phosphorylation of GSK3- β via PI3 K/Akt signaling in oral squamous cell carcinoma. *Oral Surg Oral Med Oral Pathol Oral Radiol.* 2016;122(6):719–s730. doi:10.1016/j.oooo.2016.06.008.
166. Yokoi, T, Homma, H, Odajima, T. Establishment and characterization of OSC-19 cell line in serum and protein free culture. *Tumor Res.* 1988;24:1–17.
167. Shibata, A, et al. Synthetic terrein inhibits progression of head and neck cancer by suppressing angiogenin production. *Anticancer Res.* 2016;36(5):2161–8.
168. Kawasaki, G, et al. Overexpression of metastasis-associated MTA1 in oral squamous cell carcinomas: correlation with metastasis and invasion. *Int J Oral Maxillofac Surg.* 2008;37(11):1039–46. doi:10.1016/j.ijom.2008.05.020.
169. Kamino, Y, et al. HBD-2 is downregulated in oral carcinoma cells by DNA hypermethylation, and increased expression of hBD-2 by DNA demethylation and gene transfection inhibits cell proliferation and invasion. *Oncol Rep.* 2014;32(2):462–s8. doi:10.3892/or.2014.3260.
170. Kitahara, H, et al. Eribulin sensitizes oral squamous cell carcinoma cells to cetuximab via induction of mesenchymal-to-epithelial transition. *Oncol Rep.* 2016;36(6):3139–44. doi:10.3892/or.2016.5189.
171. Yokoi, T, et al. Some properties of a newly established human cell line derived from an oral squamous carcinoma. *Tumor Res.* 1990;25(93):91–93.
172. Todoroki, K, et al. CD44v3+/CD24- cells possess cancer stem cell-like properties in human oral squamous cell carcinoma. *Int J Oncol.* 2016;48(1):99–109. doi:10.3892/ijo.2015.3261.
173. Urade, M, et al. Establishment of human squamous carcinoma cell lines highly and minimally sensitive to bleomycin and analysis of factors involved in the sensitivity. *Cancer.* 1992;69(10):2589–97. doi:10.1002/1097-0142(19920515)69:10%3c2589::AID-CNCR2820691032%3e3.0.CO;2-Y.
174. Yazama, H, et al. Dietary glucosylceramides suppress tumor growth in a mouse xenograft model of head and neck squamous cell carcinoma by the inhibition of angiogenesis through an increase in ceramide. *Int J Clin Oncol.* 2015;20(3):438–46. doi:10.1007/s10147-014-0734-y.
175. Tamura, T, et al. Zoledronic acid, a third-generation bisphosphonate, inhibits cellular growth and induces apoptosis in oral carcinoma cell lines. *Oncol Rep.* 2011;25(4):1139–43. doi:10.3892/or.2011.1152.
176. Kitano, H, et al. Long-term gene therapy with Dell fragment using nonviral vectors in mice with explanted tumors. *Onco Targets Ther.* 2016;9:503–16.
177. Berndt, A, et al. Oral squamous cell carcinoma invasion is associated with a laminin-5 matrix re-organization but independent of basement membrane and hemidesmosome formation. clues from an in vitro invasion model. *Invasion Metastasis.* 1997;17(5):251–8.
178. Palmerini, CA, et al. Synthesis of new indole-based bisphosphonates and evaluation of their chelating ability in PE/CA-PJ15 cells. *Eur J Med Chem.* 2015;102:403–12. doi:10.1016/j.ejmech.2015.08.019.
179. Lopez Jornet, P, et al. Zoledronic acid and irradiation in oral squamous cell carcinoma. *J Oral Pathol Med.* 2015;44(2):103–8. doi:10.1111/jop.12205.
180. Büttner, R, et al. Myofibroblasts have an impact on expression, dimerization and signaling of different ErbB receptors in OSCC cells. *J Recept Signal Transduct Res.* 2016;37(1):25–37. doi:10.3109/10799893.2016.1155066.
181. Jo, JR, Park, YK, Jang, BC. Short-term treatment with glucosamine hydrochloride specifically downregulates hypoxia-inducible factor-1 α at the protein level in YD-8 human tongue cancer cells. *Int J Oncol.* 2014;44(5):1699–706. doi:10.3892/ijo.2014.2336.
182. Jung, CW, et al. Anti-cancer properties of glucosamine-hydrochloride in YD-8 human oral cancer cells: Induction of the caspase-dependent apoptosis and down-regulation of HIF-1 α . *Toxicol In Vitro.* 2012;26(1):42–50. doi:10.1016/j.tiv.2011.10.005.
183. So, KY, Oh, SH. Heme oxygenase-1-mediated apoptosis under cadmium-induced oxidative stress is regulated by autophagy, which is sensitized by tumor suppressor p53. *Biochem Biophys Res Commun.* 2016;479(1):80–5. doi:10.1016/j.bbrc.2016.09.037.
184. Ahn, SG, et al. The anticancer mechanism of 2'-hydroxycinnamaldehyde in human head and neck cancer cells. *Int J Oncol.* 2015;47(5):1793–800. doi:10.3892/ijo.2015.3152.
185. Anh, TD, et al. The histone deacetylase inhibitor, Trichostatin A, induces G2/M phase arrest and apoptosis in YD-10B oral squamous carcinoma cells. *Oncol Rep.* 2012;27(2):455–60.
186. Yu, HJ, et al. Inhibition of myeloid cell leukemia-1: Association with sorafenib-induced apoptosis in human mucoepidermoid carcinoma cells and tumor xenograft. *Head Neck.* 2015;37(9):1326–35. doi:10.1002/hed.23749.
187. Kang, HJ, Jang, YJ. Selective apoptotic effect of Zerkova serrata twig extract on mouth epidermoid carcinoma through p53 activation. *Int J Oral Sci.* 2012;4(2):78–84. doi:10.1038/ijos.2012.14.
188. Lim, W, et al. Association between cancer stem cell-like properties and epithelial-to-mesenchymal transition in primary and secondary cancer cells. 2016;49(3):991–1000.
189. Rheinwald, JG, Beckett, MA. Defective terminal differentiation in culture as a consistent and selectable character of malignant human keratinocytes. *Cell.* 1980;22(2.2):629–32. doi:10.1016/0092-8674(80)90373-6.
190. Sun, L, et al. MicroRNA-137 suppresses tongue squamous carcinoma cell proliferation, migration and invasion. *Cell Prolif.* 2016;49(5):628–35. doi:10.1111/cpr.12287.

191. Su, CC, et al. Cantharidin induced oral squamous cell carcinoma cell apoptosis via the JNK-Regulated mitochondria and endoplasmic reticulum stress-related signaling pathways. *PLoS One*. 2016;11(12):e0168095. doi:10.1371/journal.pone.0168095.
192. Dai, D, et al. Inhibition of mTOR/eIF4E by anti-viral drug ribavirin effectively enhances the effects of paclitaxel in oral tongue squamous cell carcinoma. *Biochem Biophys Res Commun*. 2016;482(4):1259–1264. doi:10.1016/j.bbrc.2016.12.025.
193. Jin, L, et al. Icaritin induces mitochondrial apoptosis by up-regulating miR-124 in human oral squamous cell carcinoma cells. *Biomed Pharmacother*. 2016;85:287–295. doi:10.1016/j.biopha.2016.11.023.
194. Korvala, J, et al. MicroRNA and protein profiles in invasive versus non-invasive oral tongue squamous cell carcinoma cells in vitro. *Exp Cell Res*. 2016;350(1):9–18. doi:10.1016/j.yexcr.2016.10.015.
195. Zhang, H, et al. HMGA2 is associated with the aggressiveness of tongue squamous cell carcinoma cells. *Oral Dis*. 2016;23(2):255–264. doi:10.1111/odi.12608.
196. Gustafson, DL, et al. Dose scheduling of the dual VEGFR and EGFR tyrosine kinase inhibitor vandetanib (ZD6474, Zactima) in combination with radiotherapy in EGFR-positive and EGFR-null human head and neck tumor xenografts. *Cancer Chemother Pharmacol*. 2008;61(2):179–88. doi:10.1007/s00280-007-0460-5.
197. Bradshaw-Pierce, EL, et al. Pharmacokinetic-directed dosing of vandetanib and docetaxel in a mouse model of human squamous cell carcinoma. *Mol Cancer Ther*. 2008;7(9):3006–17. doi:10.1158/1535-7163.MCT-08-0370.
198. Bais, MV, Kukuruzinska, M, Trackman, PC. Orthotopic non-metastatic and metastatic oral cancer mouse models. *Oral Oncol*. 2015;51(5):476–82. doi:10.1016/j.oraloncology.2015.01.012.
199. Harada, K, Ferdous, T, Ueyama, Y. Gimeracil exerts radiosensitizing effects on oral squamous cell carcinoma cells in vitro and in vivo. *Anticancer Res*. 2016;36(11):5923–30. doi:10.21873/anticancer.11179.
200. Ohnishi, Y, et al. Lapatinib-resistant cancer cells possessing epithelial cancer stem cell properties develop sensitivity during sphere formation by activation of the ErbB/AKT/cyclin D2 pathway. *Oncol Rep*. 2016;36(5):3058–64. doi:10.3892/or.2016.5073.
201. Horikoshi, M, et al. A new human cell line derived from human carcinoma of the gingiva. I. Its establishment and morphological studies. *Nihon Koku Geka Gakkai Zasshi*. 1974;20(2):100–6. Article in Japanese.
202. Tsubaki, M, et al. The sensitivity of head and neck carcinoma cells to statins is related to the expression of their Ras expression status, and statin-induced apoptosis is mediated via suppression of the Ras/ERK and Ras/mTOR pathways. *Clin Exp Pharmacol Physiol*. 2016;44(2):222–234. doi:10.1111/1440-1681.12690.
203. Kudo, Y, et al. Establishment of an oral squamous cell carcinoma cell line with high invasive and p27 degradation activities from a lymph node metastasis. *Oral Oncol*. 2003;39(5):515–20. doi:10.1016/S1368-8375(03)00015-0.
204. Kudo, Y, et al. Establishment and characterization of a spindle cell squamous carcinoma cell line. 2006;35(8):479–83.
205. Inagaki, T, et al. treatment, Establishment of human oral-cancer cell lines (KOSC-2 and -3) carrying p53 and c-myc abnormalities by geneticin. *Int J Cancer*. 1994;56(2):301–8. doi:10.1002/ijc.2910560226.
206. Maemoto, S, et al. Mutational analysis of HRAS and KRAS genes in oral carcinoma cell lines. *Odontology*. 2012;100(2):149–55. doi:10.1007/s10266-011-0032-3.
207. Oyama, G, et al. Single nucleotide polymorphisms of mucosa-associated lymphoid tissue 1 in oral carcinoma cells and gingival fibroblasts. *Odontology*. 2013;101(2):150–5. doi:10.1007/s10266-012-0079-9.
208. Uozumi, M, et al. Induction of S100A4 gene expression inhibits in vitro invasiveness of human squamous cell carcinoma, KOSC-3 cells. *Cancer Lett*. 2000;149(1–2):135–41. doi:10.1016/S0304-3835(99)00352-3.
209. Chiu, KC, et al. Polarization of tumor-associated macrophages and Gas6/Axl signaling in oral squamous cell carcinoma. *Oral Oncol*. 2015;51(7):683–9. doi:10.1016/j.oraloncology.2015.04.004.
210. Yu, XD, et al. Resveratrol inhibits oral squamous cell carcinoma through induction of apoptosis and G2/M phase cell cycle arrest. *Tumour Biol*. 2016;37(3):2871–7. doi:10.1007/s13277-015-3793-4.
211. Yang, CY, Meng, CL. Regulation of PG synthase by EGF and PDGF in human oral, breast, stomach, and fibrosarcoma cancer cell lines. *J Dent Res*. 1994;73(8):1407–15. doi:10.1177/00220345940730080301.
212. Tu, HP, et al. Cyclosporine A enhances apoptosis in gingival keratinocytes of rats and in OECM1 cells via the mitochondrial pathway. *J Periodontal Res*. 2009;44:6. doi:10.1111/j.1600-0765.2008.01189.x.
213. Chang, KP, et al. Overexpression of caldesmon is associated with lymph node metastasis and poorer prognosis in patients with oral cavity squamous cell carcinoma. *Cancer*. 2013;119(22):4003–11. doi:10.1002/cncr.28300.
214. Chiang, CH, et al. Proteomics Analysis Reveals Involvement of Krt17 in Areca Nut-Induced Oral Carcinogenesis. *J Proteome Res*. 2016;15(9):2981–97. doi:10.1021/acs.jproteome.6b00138.
215. Shirako, Y, et al. Heterogeneous tumor stromal microenvironments of oral squamous cell carcinoma cells in tongue and nodal metastatic lesions in a xenograft mouse model. *J Oral Pathol Med*. 2015;44(9):656–68. doi:10.1111/jop.12318.
216. Dickson, MA, et al. Human keratinocytes that express hTERT and also bypass a p16(INK4a)-enforced mechanism that limits life span become immortal yet retain normal growth and differentiation characteristics. *Mol Cell Biol*. 2000;20(4):1436–47. doi:10.1128/MCB.20.4.1436-1447.2000.
217. Dalley, AJ, et al. Expression of ABCG2 and Bmi-1 in oral potentially malignant lesions and oral squamous

- cell carcinoma. *Cancer Med.* 2014;3(2):273–83. doi:10.1002/cam4.182.
218. Saito, Y, et al. ALY as a potential contributor to metastasis in human oral squamous cell carcinoma. *J Cancer Res Clin Oncol.* 2013;139(4):585–94. doi:10.1007/s00432-012-1361-5.
219. Roblegg, E, et al. Evaluation of a physiological in vitro system to study the transport of nanoparticles through the buccal mucosa. *Nanotoxicology.* 2012;6(4):399–413. doi:10.3109/17435390.2011.580863.
220. Konopka, K, et al. Correlation between the levels of survivin and survivin promoter-driven gene expression in cancer and non-cancer cells. *Cell Mol Biol Lett.* 2009;14(1):70–89. doi:10.2478/s11658-008-0034-5.
221. Best, M, et al. Characterisation and cytotoxic screening of metal oxide nanoparticles putative of interest to oral healthcare formulations in non-keratinised human oral mucosa cells in vitro. *Toxicol In Vitro.* 2015;30(1. B):402–11. doi:10.1016/j.tiv.2015.09.022.
222. Gokulan, R, Halagowder, D. Expression pattern of Notch intracellular domain (NICD) and Hes-1 in pre-neoplastic and neoplastic human oral squamous epithelium: their correlation with c-Myc, clinicopathological factors and prognosis in Oral cancer. *Med Oncol.* 2014;31:8. doi:10.1007/s12032-014-0126-1.
223. Pring, M, et al. Dysregulated TGF-beta1-induced Smad signalling occurs as a result of defects in multiple components of the TGF-beta signalling pathway in human head and neck carcinoma cell lines. *Int J Oncol.* 2006;28:5.
224. Ravindran, G, et al. Association of differential β -catenin expression with Oct- 4 and Nanog in oral squamous cell carcinoma and their correlation with clinicopathological factors and prognosis. *Head Neck.* 2015; 37(7):982–93. doi:10.1002/hed.23699.
225. O'Neill, ID. Continued misrepresentation of KB cells as being of oral cancer phenotype requires action. *Oral Oncol.* 2009;45(10):e117–8. doi:10.1016/j.oraloncology.2009.02.005.
226. Eagle, H. Propagation in a fluid medium of a human epidermoid carcinoma, strain KB. *Proc Soc Exp Biol Med.* 1955;89(3):362–4. doi:10.3181/00379727-89-21811.
227. Karthikeyan, S, et al. Glaucaurubinone sensitizes KB cells to paclitaxel by inhibiting ABC transporters via ROS-dependent and p53-mediated activation of apoptotic signaling pathways. *Oncotarget.* 2016;7 (27):42353–73. doi:10.18632/oncotarget.9865.
228. Li, LK, et al. Goniotalamin induces cell cycle arrest and apoptosis in H400 human oral squamous cell carcinoma: A caspase-dependent mitochondrial-mediated pathway with downregulation of NF- κ B. *Arch Oral Biol.* 2016;64:28–38. doi:10.1016/j.archoralbio.2015.12.002.
229. Khan, E, et al. Architectural characterization of organotypic cultures of H400 and primary rat keratinocytes. *J Biomed Mater Res A.* 2012;100(12):3227–38. doi:10.1002/jbm.a.34263.
230. Shaghayegh, G, et al. Cell cycle arrest and mechanism of apoptosis induction in H400 oral cancer cells in response to Damnacanthal and Nordamnacanthal isolated from *Morinda citrifolia*. *Cytotechnology.* 2016;68 (5):1999–2013. doi:10.1007/s10616-016-0014-y.
231. Lourenço, SV, et al. Establishment and characterization of an oral mucosal melanoma cell line (MEMO) derived from a longstanding primary oral melanoma. *Am J Dermatopathol.* 2013;35(2):248–51. doi:10.1097/DAD.0b013e31826a9905.
232. Zhao, M, et al. Assembly and initial characterization of a panel of 85 genomically validated cell lines from diverse head and neck tumor sites. *Clin Cancer Res.* 2011;17(23):7248–64. doi:10.1158/1078-0432.CCR-11-0690.
233. Sacks, PG, et al. Establishment and characterization of two new squamous cell carcinoma cell lines derived from tumors of the head and neck. *Cancer Res.* 1988;48(10):2858–66.
234. Xi, S, et al. Decreased STAT1 expression by promoter methylation in squamous cell carcinogenesis. *J Natl Cancer Inst.* 2006;98(3):181–9. doi:10.1093/jnci/djj020.
235. Zweifel, BS, et al. Direct evidence for a role of cyclooxygenase 2-derived prostaglandin E2 in human head and neck xenograft tumors. *Cancer Res.* 2002; 62(22):6706–11.
236. Li, C, et al. Dasatinib blocks cetuximab- and radiation-induced nuclear translocation of the epidermal growth factor receptor in head and neck squamous cell carcinoma. *Radiother Oncol.* 2010;97(2):330–7. doi:10.1016/j.radonc.2010.06.010.
237. Rangan, SR. A new human cell line (FaDu) from a hypopharyngeal carcinoma. *Cancer.* 1972;29(1):117–21. doi:10.1002/1097-0142(197201)29:1%3c117::AID-CNCR2820290119%3e3.0.CO;2-R.
238. Schneider, S, et al. Effects of neratinib and combination with irradiation and chemotherapy in head and neck cancer cells. *Oral Dis.* 2016;22(8):797–804. doi:10.1111/odi.12552.
239. Yang, SW, et al. MART-10, a newly synthesized vitamin D analog, represses metastatic potential of head and neck squamous carcinoma cells. *Drug Des Devel Ther.* 2016;10:1995–2002.
240. Chiu YW, et al. Tyrosine 397 phosphorylation is critical for FAK-promoted Rac1 activation and invasive properties in oral squamous cell carcinoma cells. *Lab Invest.* 2016;96(3):296–306. doi:10.1038/labinvest.2015.151.
241. Kawamata H, et al. Possible contribution of active MMP2 to lymph-node metastasis and secreted cathepsin L to bone invasion of newly established human oral-squamous-cancer cell lines. *Int J Cancer.* 1997; 70(1):120–7. doi:10.1002/(SICI)1097-0215(19970106)70:1%3c120::AID-IJC18%3e3.0.CO;2-P.
242. Tada T, et al. Oral squamous cell carcinoma cells modulate osteoclast function by RANKL-dependent and -independent mechanisms. *Cancer Lett.* 2009; 274(1):126–31. doi:10.1016/j.canlet.2008.09.015.

243. Erdem NF, Carlson ER, Gerard DA. Characterization of gene expression profiles of 3 different human oral squamous cell carcinoma cell lines with different invasion and metastatic capacities. *J Oral Maxillofac Surg.* 2008;66(5):918–27. doi:10.1016/j.joms.2007.12.036.
244. Kraus D, et al. Ghrelin promotes oral tumor cell proliferation by modifying GLUT1 expression. *Cell Mol Life Sci.* 2016;73(6):1287–99. doi:10.1007/s00018-015-2048-2.
245. Harada K, et al. Induction of artificial cancer stem cells from tongue cancer cells by defined reprogramming factors. *BMC Cancer.* 2016;16, 548. doi:10.1186/s12885-016-2416-9.
246. Ishisaki A, et al. Identification and characterization of autocrine-motility-factor-like activity in oral squamous-cell-carcinoma cells. *Int J Cancer.* 1994;59(6):783–8. doi:10.1002/ijc.2910590613.
247. Nguyen PT, et al. The FGFR1 inhibitor PD173074 induces mesenchymal-epithelial transition through the transcription factor AP-1. *Br J Cancer.* 2013;109(8):2248–58. doi:10.1038/bjc.2013.550.
248. Sakha S, et al. Exosomal microRNA miR-1246 induces cell motility and invasion through the regulation of DENND2D in oral squamous cell carcinoma. *Sci Rep.* 2016;6:38750. doi:10.1038/srep38750.
249. Heo DS, et al. Biology, cytogenetics, and sensitivity to immunological effector cells of new head and neck squamous cell carcinoma lines. *Cancer Res.* 1989;49(18):5167–75.
250. Minhas KM, et al. Spindle assembly checkpoint defects and chromosomal instability in head and neck squamous cell carcinoma. *Int J Cancer.* 2003;107(1):46–52. doi:10.1002/ijc.11341.
251. Brenner JC, et al. Genotyping of 73 UM-SCC head and neck squamous cell carcinoma cell lines. *Head Neck.* 2010;32(4):417–26.
252. Dickman CT, et al. Molecular characterization of immortalized normal and dysplastic oral cell lines. *J Oral Pathol Med.* 2015;44(5):329–36. doi:10.1111/jop.12236.
253. Hansson A, et al. Analysis of proliferation, apoptosis and keratin expression in cultured normal and immortalized human buccal keratinocytes. *Eur J Oral Sci.* 2003;111(1):34–41. doi:10.1034/j.1600-0722.2003.00010.x.
254. Gröger S, Michel J, Meyle J. Establishment and characterization of immortalized human gingival keratinocyte cell lines. *J Periodontal Res.* 2008;43(6):604–14. doi:10.1111/j.1600-0765.2007.01019.x.
255. Gröger S, et al. Effects of *Porphyromonas gingivalis* infection on human gingival epithelial barrier function in vitro. *Eur J Oral Sci.* 2010;118(6):582–9. doi:10.1111/j.1600-0722.2010.00782.x.
256. Gröger S, et al. Influence of retinoic acid on human gingival epithelial barriers. *J Periodontal Res.* 2016;51(6):748–57. doi:10.1111/jre.12351.
257. Hatakeyama S, et al. Establishment of gingival epithelial cell lines from transgenic mice harboring temperature sensitive simian virus 40 large T-antigen gene. *J Oral Pathol Med.* 2001;30(5):296–304. doi:10.1034/j.1600-0714.2001.300507.x.
258. Hatakeyama S, Ishida K, Takeda Y. Changes in cell characteristics due to retinoic acid; specifically, a decrease in the expression of claudin-1 and increase in claudin-4 within tight junctions in stratified oral keratinocytes. *J Periodontal Res.* 2010;45(2):207–15. doi:10.1111/j.1600-0765.2009.01219.x.
259. Hatakeyama S, et al. Expression of connexins and the effect of retinoic acid in oral keratinocytes. *J Oral Sci.* 2011;53(3):327–32. doi:10.2334/josnusd.53.327.
260. Hatakeyama S, et al. Retinoic acid disintegrated desmosomes and hemidesmosomes in stratified oral keratinocytes. *J Oral Pathol Med.* 2004;33(10):622–8. doi:10.1111/j.1600-0714.2004.00245.x.
261. Damek-Poprawa M, et al. Cell junction remodeling in gingival tissue exposed to a microbial toxin. *J Dent Res.* 2013;92(6):518–23. doi:10.1177/0022034513486807.
262. Li S, et al. *P. gingivalis* modulates keratinocytes through FOXO transcription factors. *PLoS One.* 2013;8:11.
263. Dickinson BC, et al. Interaction of oral bacteria with gingival epithelial cell multilayers. *Mol Oral Microbiol.* 2011;26(3):210–20. doi:10.1111/j.2041-1014.2011.00609.x.
264. Katz J, et al. Characterization of *Porphyromonas gingivalis*-induced degradation of epithelial cell junctional complexes. *Infect Immun.* 2000;68(3):1441–9. doi:10.1128/IAI.68.3.1441-1449.2000.
265. Meyle J, et al. Transepithelial electrical resistance and tight junctions of human gingival keratinocytes. *J Periodontal Res.* 1999;34(4):214–22. doi:10.1111/j.1600-0765.1999.tb02244.x.
266. Belibasakis GN, et al. The expression of gingival epithelial junctions in response to subgingival biofilms. *Virulence.* 2015;6(7):704–9. doi:10.1080/21505594.2015.1081731.
267. Ilmarinen T, et al. Towards a defined, serum- and feeder-free culture of stratified human oral mucosal epithelium for ocular surface reconstruction. *Acta Ophthalmol.* 2013;91(8):744–50. doi:10.1111/j.1755-3768.2012.02523.x.
268. Shimazaki J, et al. Barrier function of cultivated limbal and oral mucosal epithelial cell sheets. *Invest Ophthalmol Vis Sci.* 2009;50(12):5672–80. doi:10.1167/iovs.09-3820.
269. Kimura T, et al. Transport of D-glucose across cultured stratified cell layer of human oral mucosal cells. *JPP.* 2002;(54):213–9. doi:10.1211/0022357021778402.
270. Iida T, et al. Development of a tissue-engineered human oral mucosa equivalent based on an acellular allogeneic dermal matrix: a preliminary report of clinical application to burn wounds. *Scand J Plast Reconstr Surg Hand Surg.* 2005;39(3):138–46. doi:10.1080/0284431051006376.
271. Nakamura T, Kinoshita S. Ocular surface reconstruction using cultivated mucosal epithelial stem cells. *Cornea.* 2003;22(7 Suppl):S75–80. doi:10.1097/00003226-200310001-00011.

272. Dobrowolski D, et al. Cultivated oral mucosa epithelium in ocular surface reconstruction in aniridia patients. *Biomed Res Int.* 2015;2015, 281870. doi:10.1155/2015/281870.
273. Bhargava S, et al. Tissue-engineered buccal mucosa urethroplasty-clinical outcomes. *Eur Urol.* 2008;53(6):1263–9. doi:10.1016/j.eururo.2008.01.061.
274. Xie M, et al. Tissue-engineered buccal mucosa using silk fibroin matrices for urethral reconstruction in a canine model. *J Surg Res.* 2014;188(1):1–7. doi:10.1016/j.jss.2013.11.1102.
275. Moharamzadeh K, et al. Tissue-engineered oral mucosa: a review of the scientific literature. *J Dent Res.* 2007;86(2):115–24. doi:10.1177/154405910708600203.
276. Moharamzadeh K, et al. Tissue-engineered oral mucosa. *J Dent Res.* 2012;91(7):642–50. doi:10.1177/0022034511435702.
277. Kinikoglu B, Damour O, Hasirci V. Tissue Engineering of Oral Mucosa: A Shared Concept With Skin. *Journal of Artificial Organs.* 2015;18(1):8–19. doi:10.1007/s10047-014-0798-5.
278. Nor NH, et al. Properties of cell sources in tissue-engineered three dimensional oral mucosa model: A Review. *Curr Stem Cell Res Ther.* 2017;12(1):52–60.
279. Kosten IJ, et al. MUTZ-3 Langerhans cell maturation and CXCL12 independent migration in reconstructed human gingiva. *ALTEX.* 2016;33(4):423–34.
280. Heller M, et al. Tissue engineered pre-vascularized buccal mucosa equivalents utilizing a primary triculture of epithelial cells, endothelial cells and fibroblasts. *Biomaterials.* 2016;77:207–15. doi:10.1016/j.biomaterials.2015.10.073.
281. Dongari-Bagtzoglou A, Kashleva H. Development of a highly reproducible three-dimensional organotypic model of the oral mucosa. *Nat Protoc.* 2006;1(4):2012–8. doi:10.1038/nprot.2006.323.
282. Ceder R, et al. Differentiation-promoting culture of competent and noncompetent keratinocytes identifies biomarkers for head and neck cancer. *Am J Pathol.* 2012;180(2):457–72. doi:10.1016/j.ajpath.2011.10.016.
283. Chakravarti N, et al. Differential inhibition of protein translation machinery by curcumin in normal, immortalized, and malignant oral epithelial cells. *Cancer Prev Res (Phila).* 2010;3(3):331–8. doi:10.1158/1940-6207.CAPR-09-0076.
284. Parikh N, et al. Isolation and characterization of an immortalized oral keratinocyte cell line of mouse origin. *Arch Oral Biol.* 2008;53(11):1091–100. doi:10.1016/j.archoralbio.2008.07.002.
285. Conti HR, et al. IL-17 Receptor Signaling in Oral Epithelial Cells Is Critical for Protection against Oropharyngeal Candidiasis. *Cell Host & Microbe.* 2016;20(5):606–17. doi:10.1016/j.chom.2016.10.001.
286. Takahashi C, et al. Newly established cell lines from mouse oral epithelium regenerate teeth when combined with dental mesenchyme. *In Vitro Cell Dev Biol Anim.* 2010;46(5):457–68. doi:10.1007/s11626-009-9265-7.
287. Mäkelä M, Salo T, Larjava H. MMP-9 from TNF alpha-stimulated keratinocytes binds to cell membranes and type I collagen: a cause for extended matrix degradation in inflammation? *Biochem Biophys Res Commun.* 1998;253(2):325–35. doi:10.1006/bbrc.1998.9641.
288. Hildebrand HC, et al. Characterization of organotypic keratinocyte cultures on de-epithelialized bovine tongue mucosa. *Histol Histopathol.* 2002;17(1):151–63.
289. Turunen A, et al. The combined effects of irradiation and herpes simplex virus type 1 infection on an immortal gingival cell line. *Virol J.* 2014;11, 125. doi:10.1186/1743-422X-11-125.
290. Turunen A, Syrjänen S. Extracellular calcium regulates keratinocyte proliferation and HPV 16 E6 RNA expression in vitro. *APMIS.* 2014;122(9):781–9. doi:10.1111/apm.12227.
291. Gursoy UK, et al. Construction and characterization of a multilayered gingival keratinocyte culture model: the TURK-U model. *Cytotechnology.* 2016;68(6):2345–54. doi:10.1007/s10616-016-0029-4.
292. Oda D, et al. HPV immortalization of human oral epithelial cells: a model for carcinogenesis. *Exp Cell Res.* 1996;226(1):164–9. doi:10.1006/excr.1996.0215.
293. Parikka M, et al. Alterations of collagen XVII expression during transformation of oral epithelium to dysplasia and carcinoma. *J Histochem Cytochem.* 2003;51(7):921–9. doi:10.1177/002215540305100707.
294. Lee HJ, et al. Effects of nicotine on proliferation, cell cycle, and differentiation in immortalized and malignant oral keratinocytes. *J Oral Pathol Med.* 2005;34(7):436–43. doi:10.1111/j.1600-0714.2005.00342.x.
295. Roesch-Ely M, et al. Organotypic co-cultures allow for immortalized human gingival keratinocytes to reconstitute a gingival epithelial phenotype in vitro. *Differentiation.* 2006;74(9–10):622–37. doi:10.1111/j.1432-0436.2006.00099.x.
296. Buskermolen JK, et al. Development of a full-thickness human gingiva equivalent constructed from immortalized keratinocytes and fibroblasts. *Tissue Eng Part C Methods.* 2016;22(8):781–91. doi:10.1089/ten.tec.2016.0066.
297. Kibe T, et al. Immortalization and characterization of normal oral epithelial cells without using HPV and SV40 genes. *Oral Science International.* 2011;8(1):20–28. doi:10.1016/S1348-8643(11)00009-7.
298. Miyata K, Takebe J. Anodized-hydrothermally treated titanium with a nanopopographic surface structure regulates integrin- $\alpha 6\beta 4$ and laminin-5 gene expression in adherent murine gingival epithelial cells. *J Prosthodont Res.* 2013;57(2):99–108. doi:10.1016/j.jprr.2012.12.002.
299. Nakayama Y, et al. Amelotin gene expression is temporarily being upregulated at the initiation of apoptosis induced by TGF $\beta 1$ in mouse gingival epithelial cells.

- Apoptosis. 2016;21(10):1057–70. doi:10.1007/s10495-016-1279-5.
300. Moffatt-Jauregui, CE, et al. Establishment and characterization of a telomerase immortalized human gingival epithelial cell line. *J Periodontal Res.* 2013;48(6):713–21.
301. Jauregui, CE, et al. Suppression of T-Cell Chemokines by *Porphyromonas gingivalis*. *Infect Immun.* 2013; 81(7):2288–95. doi:10.1128/IAI.00264-13.
302. Takeuchi, H, et al. The serine phosphatase SerB of *Porphyromonas gingivalis* suppresses IL-8 production by dephosphorylation of NF- κ B RelA/p65. *PLoS Pathog.* 2013;9(4):e1003326. doi:10.1371/journal.ppat.1003326.
303. Wang, H, et al. *Porphyromonas gingivalis*-induced reactive oxygen species activate JAK2 and regulate production of inflammatory cytokines through c-Jun. *Infect Immun.* 2014;82(10):4118–26. doi:10.1128/IAI.02000-14.
304. Chen, SC, et al. MicroRNAs regulate cytokine responses in gingival epithelial cells. *Infect Immun.* 2016;84(12):3282–9. doi:10.1128/IAI.00263-16.
305. Bao, K, Akguel, B, Bostanci, N. Establishment and characterization of immortalized gingival epithelial and fibroblastic cell lines for the development of organotypic cultures. *Cells Tissues Organs.* 2014;199(4):228–37. doi:10.1159/000363694.
306. Kubo, C, et al. Immortalization of normal human gingival keratinocytes and cytological and cytogenetic characterization of the cells. *Odontology.* 2009;97(1):18–31. doi:10.1007/s10266-008-0089-9.
307. Kusumoto, Y, et al. Human gingival epithelial cells produce chemotactic factors interleukin-8 and monocyte chemoattractant protein-1 after stimulation with *Porphyromonas gingivalis* via toll-like receptor 2. *J Periodontol.* 2004;75(3):370–9. doi:10.1902/jop.2004.75.3.370.
308. Umeda, JE, et al. Differential transcription of virulence genes in *Aggregatibacter actinomycetemcomitans* serotypes. *J Oral Microbiol.* 2013;5. doi:10.3402/jom.v5i0.21473.
309. Savitri, IJ, et al. Irsogladine maleate inhibits *Porphyromonas gingivalis*-mediated expression of toll-like receptor 2 and interleukin-8 in human gingival epithelial cells. *J Periodontal Res.* 2015;50(4):486–93. doi:10.1111/jre.12231.
310. Ouhara, K, et al. miR-584 expressed in human gingival epithelial cells is induced by *Porphyromonas gingivalis* stimulation and regulates interleukin-8 production via lactoferrin receptor. *J Periodontol.* 85, 2014;6:e198–204. doi:10.1902/jop.2013.130335.
311. Benso, B, et al. *Malva sylvestris* inhibits inflammatory response in oral human cells. *An In Vitro Infection Model.* *PLoS One.* 2015;10(10):e0140331. doi:10.1371/journal.pone.0140331.
312. Castilho, et al. Rac1 is required for epithelial stem cell function during dermal and oral mucosal wound healing but not for tissue homeostasis in mice. 2010;5(5):e10503.
313. Glazer, CA, et al. The Role of MAGEA2 in head and neck cancer. *Arch Otolaryngol Head Neck Surg.* 2011;137(3):286–93. doi:10.1001/archoto.2011.2.
314. Bhan, S, et al. MAGEA4 induces growth in normal oral keratinocytes by inhibiting growth arrest and apoptosis. *Oncol Rep.* 2012;28(4):1498–502. doi:10.3892/or.2012.1934.
315. Pelliccioli, AC, et al. Laser phototherapy accelerates oral keratinocyte migration through the modulation of the mammalian target of rapamycin signaling pathway. *J Biomed Opt.* 2014;19(2):028002. doi:10.1117/1.JBO.19.2.028002.
316. Martins, MD, et al. Epigenetic modifications of histones in periodontal disease. *J Dent Res.* 2016;95(2):215–22. doi:10.1177/0022034515611876.
317. Dongari-Bagtzoglou, A, Kashleva, H. *Candida albicans* triggers interleukin-8 secretion by oral epithelial cells. *Microb Pathog.* 2003;34(4):169–77. doi:10.1016/S0882-4010(03)00004-4.
318. Wöllert, T, et al. Human oral keratinocytes: a model system to analyze host-pathogen interactions. *Methods Mol Biol.* 2012;845:289–302. doi:10.1007/978-1-61779-539-8_19.
319. Volk, et al. Glutathione level and genotoxicity in human oral keratinocytes exposed to TEGDMA. *J Biomed Mater Res B Appl Biomater.* 2012;100(2):391–9. doi:10.1002/jbm.b.31960.
320. Ramage, G, et al. Antifungal, cytotoxic, and immunomodulatory properties of tea tree oil and its derivative components: potential role in management of oral candidosis in cancer patients. *Front Microbiol.* 2012;3:220. doi:10.3389/fmicb.2012.00220.
321. Millhouse, E, et al. Development of an in vitro periodontal biofilm model for assessing antimicrobial and host modulatory effects of bioactive molecules. *BMC Oral Health.* 2014;14:80. doi:10.1186/1472-6831-14-80.
322. Wessels, M, et al. Genotoxic effects of camphorquinone and DMT on human oral and intestinal cells. *Dent Mater.* 2015;31(10):1159–68. doi:10.1016/j.dental.2015.06.007.
323. Almela, T, Brook, IM, Moharamzadeh, K. Development of three-dimensional tissue engineered bone-oral mucosal composite models. *J Mater Sci Mater Med.* 2016;27:65. doi:10.1007/s10856-016-5676-7.
324. Gilchrist, EP, et al. Establishment of a human polyclonal oral epithelial cell line. *Oral Surg Oral Med Oral Pathol Oral Radiol Endod.* 2000;90(3):340–7. doi:10.1067/moe.2000.107360.
325. Kanno, F, Korostoff J, Volgina A, DiRienzo JM. Resistance of human periodontal ligament fibroblasts to the cytolethal distending toxin of *Actinobacillus actinomycetemcomitans*. *J Periodontol.* 2005;76(7):1189–201. doi:10.1902/jop.2005.76.7.1189.
326. Feghali, K, Tanabe, S, Grenier, D. Soluble CD14 induces cytokine release by human oral epithelial cells. *J Periodontal Res.* 2011;46(1):147–52. doi:10.1111/j.1600-0765.2010.01311.x.
327. Yee, M, et al. *Porphyromonas gingivalis* stimulates IL-6 and IL-8 secretion in GMSM-K, HSC-3 and H413 oral

- epithelial cells. *Anaerobe*. 2014;28:62–7. doi:10.1016/j.anaerobe.2014.05.011.
328. Tabuchi, Y, et al. Development of oral epithelial cell line ROE2 with differentiation potential from transgenic rats harboring temperature-sensitive simian virus40 large T-antigen gene. *Exp Anim*. 1, 2014;63:31–44. doi:10.1538/expanim.63.31.
 329. Tabuchi, Y, et al. Genes and gene networks involved in sodium fluoride-elicited cell death accompanying endoplasmic reticulum stress in oral epithelial cells. *Int J Mol Sci*. 2014;15(5):8959–78. doi:10.3390/ijms15058959.
 330. Eirheim, HU, Bundgaard, C, Nielsen, HM. Evaluation of different toxicity assays applied to proliferating cells and to stratified epithelium in relation to permeability enhancement with glycocholate. *Toxicol In Vitro*. 2004;18(5):649–57. doi:10.1016/j.tiv.2004.02.003.
 331. Ye, P, et al. CD24 regulated gene expression and distribution of tight junction proteins is associated with altered barrier function in oral epithelial monolayers. *BMC Cell Biol*. 2009;10:2. doi:10.1186/1471-2121-10-2.
 332. Acheampong, EA, et al. Molecular interactions of human immunodeficiency virus type 1 with primary human oral keratinocytes. *J Virol*. 2005;79(13):8440–53. doi:10.1128/JVI.79.13.8440-8453.2005.
 333. Schaal S, Kunsch K, Kunsch S. *Der Mensch in Zahlen: Eine Datensammlung in Tabellen mit über 20000 Einzelwerten*. s.l.: Springer-Verlag; 2015:506.
 334. Edgar WM. Saliva: its secretion, composition and functions. *Br Dent J*. 1992;172(8):305–12. doi:10.1038/sj.bdj.4807861.
 335. Nelson, J, Manzella, K, Baker, OJ. Current cell models for bioengineering a salivary gland: a mini-review of emerging technologies. *Oral Dis*. 2013;19(3):236–44. doi:10.1111/j.1601-0825.2012.01958.x.
 336. Maria, OM, et al. Distribution of tight junction proteins in adult human salivary glands. *J Histochem Cytochem*. 2008;56(12):1093–8. doi:10.1369/jhc.2008.951780.
 337. Baker, OJ. Tight junctions in salivary epithelium. *J Biomed Biotechnol*. 2010;2010:278948. doi:10.1155/2010/278948.
 338. Baker, OJ. Current trends in salivary gland tight junctions. *Tissue Barriers*. 2016;4:3. doi:10.1080/21688370.2016.1162348.
 339. Zhang, GH, Wu, LL, Yu, GY. Tight junctions and paracellular fluid and ion transport in salivary glands. *Chin J Dent Res*. 2013;16(1):13–46.
 340. Michikawa, H, Fujita-Yoshigaki, J, Sugiya, H. Enhancement of barrier function by overexpression of claudin-4 in tight junctions of submandibular gland cells. *Cell Tissue Res*. 2008;334(2):255–64. doi:10.1007/s00441-008-0689-2.
 341. Xiang, RL, et al. Claudin-4 is required for AMPK-modulated paracellular permeability in submandibular gland cells. *J Mol Cell Biol*. 2014;6(6):486–97. doi:10.1093/jmcb/mju048.
 342. Cong, X, et al. Claudin-4 is required for modulation of paracellular permeability by muscarinic acetylcholine receptor in epithelial cells. *J Cell Sci*. 2015;128(12):2271–86. doi:10.1242/jcs.165878.
 343. Li, D, Mrsny, RJ. Oncogenic Raf-1 disrupts epithelial tight junctions via downregulation of occludin. *J Cell Biol*. 2000;148(4):791–800. doi:10.1083/jcb.148.4.791.
 344. Hamm-Alvarez, SF, et al. Etk/Bmx activation modulates barrier function in epithelial cells. *Am J Physiol Cell Physiol*. 2001;280(6):C1657–68. doi:10.1152/ajp-cell.2001.280.6.C1657.
 345. Castro, R, et al. Ion transport in an immortalized rat submandibular cell line SMG-C6. *Proc Soc Exp Biol Med*. 2000;225(1):39–48. doi:10.1046/j.1525-1373.2000.22505.x.
 346. Aframian, DJ, et al. Absence of tight junction formation in an allogeneic graft cell line used for developing an engineered artificial salivary gland. *Tissue Eng*. 2002;8(5):871–8. doi:10.1089/10763270260424231.
 347. Maria, OM, et al. Matrigel improves functional properties of human submandibular salivary gland cell line. *Int J Biochem Cell Biol*. 2011;43(4):622–31. doi:10.1016/j.biocel.2011.01.001.
 348. Capes-Davis, A, et al. Check your cultures! A list of cross-contaminated or misidentified cell lines. *Int J Cancer*. 2010;127(1):1–8. doi:10.1002/ijc.25242.
 349. Uematsu, T, et al. Expression of ATP-binding cassette transporter in human salivary ducts. *Arch Oral Biol*. 2003;48(1):87–90. doi:10.1016/S0003-9969(02)00159-0.
 350. Matsuoka T, Aiyama S, Kikuchi KI, Koike K. Uptake of cationized ferritin by the epithelium of the main excretory duct of the rat submandibular gland. *Anat Rec*. 2000;258(1):108–13. doi:10.1002/(SICI)1097-0185(20000101)258:1%3c108::AID-AR12%3e3.0.CO;2-D.
 351. Lotti LV, Hand AR. Endocytosis of native and glycosylated bovine serum albumin by duct cells of the rat parotid gland. *Cell Tissue Res*. 1989;255(2):333–42. doi:10.1007/BF00224116.
 352. Park MY, Kim N, Wu LL, Yu GY, Park K. Role of flotillins in the endocytosis of GPCR in salivary gland epithelial cells. *Biochem Biophys Res Commun*. 2016;476(4):237–44. doi:10.1016/j.bbrc.2016.05.103.
 353. Pirraglia C, Walters J, Myat MM. Pak1 control of E-cadherin endocytosis regulates salivary gland lumen size and shape. *Development*. 2010;137(24):4177–89. doi:10.1242/dev.048827.
 354. Lisi S, Sisto M, Soleti R, Saponaro C, Scagliusi P. Fcγ receptors mediate internalization of anti-Ro and anti-La autoantibodies from Sjögren's syndrome and apoptosis in human salivary gland cell line A-253. *J Oral Pathol Med*. 2007;36(9):511–23. doi:10.1111/j.1600-0714.2007.00563.x.
 355. Liu CX, Li Y, Obermoeller-McCormick LM, Schwartz AL, Bu G. The putative tumor suppressor LRP1B, a novel member of the low density lipoprotein (LDL) receptor family, exhibits both overlapping and distinct properties with the LDL receptor-related protein. *J*

- Biol Chem. 2001;276(31):28889–96. doi:10.1074/jbc.M102727200.
356. Burghartz M, Lennartz S, Schweinlin M, Hagen R, Kleinsasser N, Hackenberg S, Steußloff G, Scherzad A, Radeloff K, Ginzkey C, et al. Development of human salivary gland-like tissue in vitro. *Tissue Eng Part A*. 2018;24(3-4):301–309. doi:10.1089/ten.tea.2016.0466.
357. Bamforth, SD, et al. A dominant mutant of occludin disrupts tight junction structure and function. *J Cell Sci*. 1999;112(12):1879–88.
358. Vogel, C, et al. Flt-1, but not Flk-1 mediates hyperpermeability through activation of the PI3-K/Akt pathway. *J Cell Physiol*. 2007;212(1):236–43. doi:10.1002/jcp.21022.
359. Mitsui, R, et al. Maintenance of paracellular barrier function by insulin-like growth factor-I in submandibular gland cells. *Arch Oral Biol*. 2010;55(12):963–9. doi:10.1016/j.archoralbio.2010.07.023.
360. He X, et al. A polarized salivary cell monolayer useful for studying transepithelial fluid movement in vitro. *Pflugers Arch*. 1998;435(3):375–81. doi:10.1007/s004240050526.
361. Li J, et al. ZO-1 and -2 Are Required for TRPV1-Modulated Paracellular Permeability. *J Dent Res*. 2015;94(12):1748–56. doi:10.1177/0022034515609268.
362. Cong X, et al. Occludin is required for TRPV1-modulated paracellular permeability in the submandibular gland. *J Cell Sci*. 2013;126(5):1109–21. doi:10.1242/jcs.111781.
363. Ding C, et al. Adiponectin increases secretion of rat submandibular gland via adiponectin receptors-mediated AMPK signaling. *PLoS One*. 2013;8(5):e63878. doi:10.1371/journal.pone.0063878.
364. Quissell DO, et al. Development and characterization of SV40 immortalized rat parotid acinar cell lines. In *Vitro Cell Dev Biol Anim*. 1998;34(1):58–67. doi:10.1007/s11626-998-0054-5.
365. Shirasuna K, Sato M, Miyazaki T. A neoplastic epithelial duct cell line established from an irradiated human salivary gland. *Cancer*. 1981;48(3):745–52. doi:10.1002/1097-0142(19810801)48:3%3c745::AID-CNCR2820480314%3e3.0.CO;2-7.
366. Sato M, et al. Search for specific markers of neoplastic epithelial duct and myoepithelial cell lines established from human salivary gland and characterization of their growth in vitro. *Cancer*. 1984;54(12):2959–67. doi:10.1002/1097-0142(19841215)54:12%3c2959::AID-CNCR2820541225%3e3.0.CO;2-5.
367. Jang SI, et al. Establishment of functional acinar-like cultures from human salivary glands. *J Dent Res*. 2015;94(2):304–11. doi:10.1177/0022034514559251.
368. Tran SD, et al. Primary culture of polarized human salivary epithelial cells for use in developing an artificial salivary gland. *Tissue Eng*. 2005;11(1-2):172–81. doi:10.1089/ten.2005.11.172.
369. Hegyesi O, et al. Evidence for active electrolyte transport by two-dimensional monolayers of human salivary epithelial cells. *Tissue Eng Part C Methods*. 2015;21(12):1226–36. doi:10.1089/ten.tec.2014.0614.
370. Maria OM, et al. Matrigel improves functional properties of primary human salivary gland cells. *Tissue Eng Part A*. 2011a;17(9–10):1229–38. doi:10.1089/ten.tea.2010.0297.
371. Szlávik V, et al. Differentiation of primary human submandibular gland cells cultured on basement membrane extract. *Tissue Eng Part A*. 2008;14(11):1915–26. doi:10.1089/ten.tea.2007.0208.
372. Tran SD, et al. Re-engineering primary epithelial cells from rhesus monkey parotid glands for use in developing an artificial salivary gland. *Tissue Eng*. 2006;12(10):2939–48. doi:10.1089/ten.2006.12.2939.
373. Aframian DJ, et al. Characterization of murine autologous salivary gland graft cells: a model for use with an artificial salivary gland. *Tissue Eng*. 2004;10(5–6):914–20. doi:10.1089/1076327041348518.